Published for SISSA by Springer

Received: January 11, 2018
Accepted: March 16, 2018
Published: March 27, 2018

Combined search for electroweak production of charginos and neutralinos in proton-proton collisions at $\sqrt{s} = 13$ TeV

The CMS collaboration

E-mail: cms-publication-committee-chair@cern.ch

Abstract: A statistical combination of several searches for the electroweak production of charginos and neutralinos is presented. All searches use proton-proton collision data at $\sqrt{s} = 13$ TeV, recorded with the CMS detector at the LHC in 2016 and corresponding to an integrated luminosity of 35.9 fb^{-1}. In addition to the combination of previous searches, a targeted analysis requiring three or more charged leptons (electrons or muons) is presented, focusing on the challenging scenario in which the difference in mass between the two least massive neutralinos is approximately equal to the mass of the Z boson. The results are interpreted in simplified models of chargino-neutralino or neutralino pair production. For chargino-neutralino production, in the case when the lightest neutralino is massless, the combination yields an observed (expected) limit at the 95% confidence level on the chargino mass of up to 650 (570) GeV, improving upon the individual analysis limits by up to 40 GeV. If the mass difference between the two least massive neutralinos is approximately equal to the mass of the Z boson in the chargino-neutralino model, the targeted search requiring three or more leptons obtains observed and expected exclusion limits of around 225 GeV on the second neutralino mass and 125 GeV on the lightest neutralino mass, improving the observed limit by about 60 GeV in both masses compared to the previous CMS result. In the neutralino pair production model, the combined observed (expected) exclusion limit on the neutralino mass extends up to 650–750 (550–750) GeV, depending on the branching fraction assumed. This extends the observed exclusion achieved in the individual analyses by up to 200 GeV. The combined result additionally excludes some intermediate gaps in the mass coverage of the individual analyses.

Keywords: Hadron-Hadron scattering (experiments), Supersymmetry

ArXiv ePrint: 1801.03957

https://doi.org/10.1007/JHEP03(2018)160

JHEP03(2018)160

Contents

1 Introduction

Supersymmetry (SUSY) [1–8] is an extension of the standard model (SM) of particle physics. It posits a new symmetry such that for each boson (fermion) in the SM, there exists a fermionic (bosonic) superpartner. Supersymmetry can potentially address several of the open questions in particle physics, including the hierarchy problem [9–11] and the unification of the gauge couplings at high energy scales [12, 13]. If R-parity [14] is conserved, the lightest SUSY particle (LSP) is stable and could be a potential dark matter candidate [15, 16].

This paper focuses on searches for electroweak production of SUSY particles, under the assumption that the strongly-coupled SUSY particles are too massive to be directly produced. The superpartners of the bosons from the SM SU(2) and U(1) gauge fields before electroweak symmetry breaking are denoted as the winos and bino, respectively. We consider SUSY models assuming two complex Higgs doublets, and the superpartners of the Higgs bosons are denoted as higgsinos. The bino, winos, and higgsinos form mass eigenstates of two charginos ($\widetilde{\chi}^{\pm}$) and four neutralinos ($\widetilde{\chi}^{0}$) and in general can mix among one another. In this paper, we focus on the lightest neutralino ($\widetilde{\chi}^{0}_{1}$), the next-to-lightest neutralino ($\widetilde{\chi}^{0}_{2}$), and the lightest chargino ($\widetilde{\chi}^{\pm}_{1}$). If the superpartners of the SM leptons, the sleptons, are much heavier than the charginos and neutralinos, decays of the charginos and neutralinos proceed through the W, Z, and Higgs bosons. The branching fractions of neutralinos to the Z and Higgs bosons depend on the mixing among the bino, winos, and higgsinos to form mass eigenstates.

Searches performed at LEP exclude promptly-decaying charginos below a mass of 103.5 GeV [17]. At the LHC, several searches have been performed by the ATLAS [18–29] and CMS [30–43] Collaborations looking for direct production of charginos and neutralinos. Given the various possible decay modes, a SUSY signal could simultaneously populate multiple final states. This paper implements a statistical combination of the searches performed by CMS in refs. [38–43] covering several final states to improve upon the sensitivity of the individual analyses, particularly in models where the neutralino has a nonzero branching fraction to both Z and Higgs bosons. In addition, we present an extension of a search selecting events with three or more charged leptons [38]. It targets the difficult region of phase space where the difference in mass between the $\widetilde{\chi}^{0}_{2}$ and $\widetilde{\chi}^{0}_{1}$ is approximately equal to the Z boson mass, and the signal has similar kinematic properties to the dominant background of SM WZ production. All searches use a data sample of LHC proton-proton collisions at $\sqrt{s} = 13\,\text{TeV}$ collected by the CMS experiment in 2016, corresponding to an integrated luminosity of 35.9 fb^{-1}.

2 Signal models

Simplified models of SUSY [44–47] are used to interpret the combined search results presented below. In this paper, "H" refers to the 125 GeV scalar boson [48], interpreted as the lightest CP-even state of an extended Higgs sector. The H boson is expected to have SM-like properties if all of the other Higgs bosons are much heavier [49]. All signal models considered involve the production of two bosons (W, Z, or H) through SUSY decays, and we denote each model by the specific bosons produced. The W, Z, and H bosons are always assumed to decay according to their SM branching fractions. The sleptons are always assumed to have much higher masses than the charginos and neutralinos such that they do not contribute to the interactions.

The first class of models assumes $\widetilde{\chi}^{\pm}_{1}\widetilde{\chi}^{0}_{2}$ production. The $\widetilde{\chi}^{0}_{1}$ is assumed to be the LSP. The $\widetilde{\chi}^{\pm}_{1}$ always decays to the W boson and the $\widetilde{\chi}^{0}_{1}$, while the $\widetilde{\chi}^{0}_{2}$ can decay to either of the Z or H bosons plus the $\widetilde{\chi}^{0}_{1}$. We consider three choices for the $\widetilde{\chi}^{0}_{2}$ decay: a branching fraction of 100% to $\text{Z}\widetilde{\chi}^{0}_{1}$ (WZ topology), of 100% to $\text{H}\widetilde{\chi}^{0}_{1}$ (WH topology), and of 50% to each of these two decays (mixed topology). This model is depicted in figure 1, showing the two possible decays. The production cross sections are computed in the limit of mass-degenerate winos $\widetilde{\chi}^{\pm}_{1}$ and $\widetilde{\chi}^{0}_{2}$, and light bino $\widetilde{\chi}^{0}_{1}$, with all other sparticles assumed to be heavy and decoupled.

The second class of models assumes $\widetilde{\chi}^{0}_{1}\widetilde{\chi}^{0}_{1}$ production. For bino- or wino-like neutralinos, the neutralino pair production cross section is very small, and thus we consider a specific gauge-mediated SUSY breaking (GMSB) model with quasidegenerate higgsi-

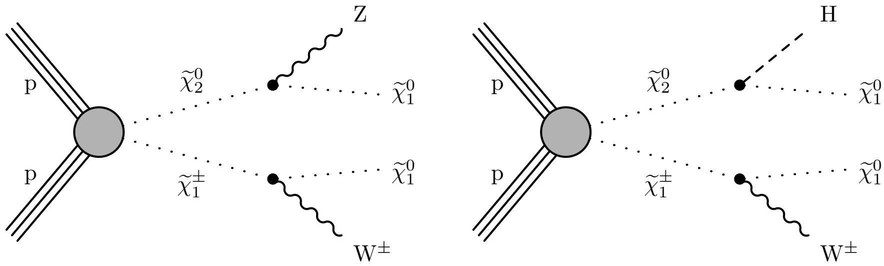

Figure 1. Production of $\widetilde{\chi}_1^\pm\widetilde{\chi}_2^0$ with the $\widetilde{\chi}_1^\pm$ decaying to a W boson and the LSP, $\widetilde{\chi}_1^0$, and the $\widetilde{\chi}_2^0$ decaying to either (left) a Z boson and the $\widetilde{\chi}_1^0$ or (right) a H boson and the $\widetilde{\chi}_1^0$.

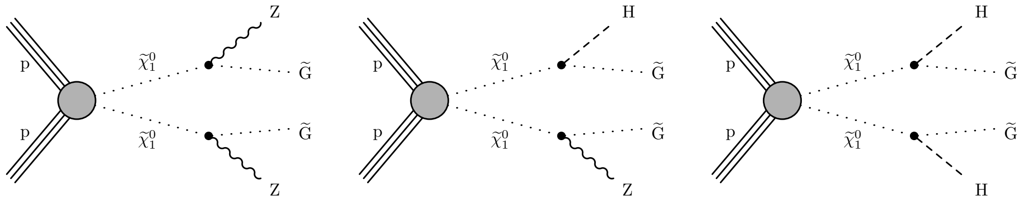

Figure 2. A GMSB model with $\widetilde{\chi}_1^0\widetilde{\chi}_1^0$ pair production. The two $\widetilde{\chi}_1^0$ particles decay into the $\widetilde{G}$ LSP and (left) both to Z bosons, (center) a Z and a H boson, or (right) both to H bosons.

nos as next-to-lightest SUSY particles and an effectively massless gravitino ($\widetilde{G}$) as the LSP [50–52]. In the production of any two of these, $\widetilde{\chi}_1^\pm$ or $\widetilde{\chi}_2^0$ decays immediately to $\widetilde{\chi}_1^0$ and low-momentum particles that do not impact the analysis, effectively yielding pair production of $\widetilde{\chi}_1^0\widetilde{\chi}_1^0$. The $\widetilde{\chi}_1^0$ then decays to a $\widetilde{G}$ and either a Z or H boson, and we consider varying branching fractions from 100% decay into the Z boson to 100% decay into the H boson including intermediate values. The possible decays in this model are shown in figure 2.

The production cross sections for the GMSB scenario are computed in a limit of mass-degenerate higgsino states $\widetilde{\chi}_1^\pm$, $\widetilde{\chi}_2^0$, and $\widetilde{\chi}_1^0$, with all the other sparticles assumed to be heavy and decoupled. Following the convention of real mixing matrices and signed neutralino masses [53], we set the sign of the mass of $\widetilde{\chi}_1^0$ ($\widetilde{\chi}_2^0$) to +1 (−1). The lightest two neutralino states are defined as symmetric (antisymmetric) combinations of higgsino states by setting the product of the elements N_{i3} and N_{i4} of the neutralino mixing matrix N to +0.5 (−0.5) for $i = 1$ (2). The elements U_{12} and V_{12} of the chargino mixing matrices U and V are set to 1.

Cross section calculations to next-to-leading order (NLO) plus next-to-leading-logarithmic (NLL) accuracy [54–59] in perturbative quantum chromodynamics (QCD) are used to normalize the signal samples for the results presented in sections 6 and 7. In this section, we present cross sections calculated to NLO accuracy [56] to demonstrate the dependence of the cross section values on assumptions made in decoupling other SUSY particles. The same qualitative conclusions also hold for the NLO+NLL calculations used in the final results.

JHEP03(2018)160

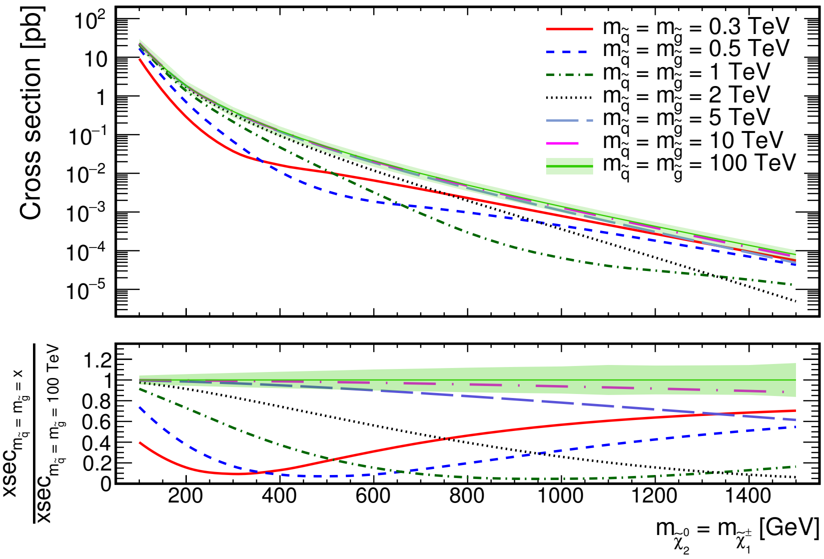

Figure 3. Cross section for $\widetilde{\chi}^{\pm}_1\widetilde{\chi}^0_2$ production at $\sqrt{s} = 13\,\text{TeV}$ versus the wino mass, calculated to NLO accuracy in QCD with RESUMMINO [56]. The $\widetilde{\chi}^{\pm}_1$ and $\widetilde{\chi}^0_2$ are assumed to be mass-degenerate winos. The various curves show different assumptions on the masses of the squarks and gluinos, as described in the legend. The green band shows the theoretical uncertainty in the cross section calculation, from the variation of renormalization and factorization scales as well as parton density functions, for the 100 TeV squark and gluino mass assumption.

Figure 3 shows the NLO cross section for $\widetilde{\chi}^{\pm}_1\widetilde{\chi}^0_2$ production at $\sqrt{s} = 13\,\text{TeV}$ assuming mass-degenerate winos $\widetilde{\chi}^{\pm}_1$ and $\widetilde{\chi}^0_2$. The various curves show different assumptions on the masses of squarks ($\widetilde{q}$) and gluinos ($\widetilde{\text{g}}$), as described in the legend. The cross section depends significantly on the masses of the strongly coupled particles until they reach masses of at least 10 TeV. For the range of $\widetilde{\chi}^{\pm}_1$ and $\widetilde{\chi}^0_2$ masses considered here, the reduction can make up to 90% in the cross section value. This is due to large destructive interference effects from t-channel diagrams involving squark exchange. The cross section calculation used in the interpretations of the analysis results assumes a mass of 100 TeV for the squarks and gluinos to have them fully decoupled. The obtained results would be less stringent if lower masses were assumed for the squarks and gluinos. We performed the same study for $\widetilde{\chi}^{\pm}_1\widetilde{\chi}^0_2$, $\widetilde{\chi}^{\pm}_1\widetilde{\chi}^0_1$, $\widetilde{\chi}^{\pm}_1\widetilde{\chi}^{\mp}_1$, and $\widetilde{\chi}^0_2\widetilde{\chi}^0_1$ production with the assumption of mass-degenerate higgsinos $\widetilde{\chi}^{\pm}_1$, $\widetilde{\chi}^0_2$, and $\widetilde{\chi}^0_1$. The dependence of the production cross section on the decoupling mass assumption was found to be much smaller in the higgsino case, at most a few percent, and it is small compared to the uncertainty in the cross section calculation.

3 The CMS detector

The central feature of the CMS apparatus is a superconducting solenoid, 13 m in length and 6 m in diameter, that provides an axial magnetic field of 3.8 T. The bore of the solenoid is outfitted with various particle detection systems. Charged-particle trajectories are measured by silicon pixel and strip trackers, covering $0 < \phi < 2\pi$ in azimuth and $|\eta| < 2.5$, where the pseudorapidity η is defined as $-\log[\tan(\theta/2)]$, with θ being the polar angle of the trajectory of the particle with respect to the clockwise beam direction. A crystal electromagnetic calorimeter (ECAL) and a brass and scintillator hadron calorimeter (HCAL) surround the tracking volume. The calorimeters provide energy and direction measurements of electrons, photons, and hadronic jets. Muons are measured in gas-ionization detectors embedded in the steel flux-return yoke outside the solenoid. The detector is nearly hermetic, allowing for energy balance measurements in the plane transverse to the clockwise beam direction. A two-tier trigger system selects the most interesting pp collision events for use in physics analysis. A more detailed description of the CMS detector, together with a definition of the coordinate system used and the relevant kinematic variables, can be found in ref. [60].

4 Event reconstruction and Monte Carlo simulation

Event reconstruction is based on the particle-flow (PF) algorithm [61], which optimally combines information from the tracker, calorimeters, and muon systems to reconstruct and identify PF candidates, i.e., charged and neutral hadrons, photons, electrons, and muons. To select collision events, we require at least one reconstructed vertex. The reconstructed vertex with the largest value of summed physics-object p_{T}^2 is taken to be the primary pp interaction vertex, where p_{T} is the transverse momentum with respect to the beam axis. The physics objects are the objects returned by a jet finding algorithm [62, 63] applied to all charged tracks associated with the vertex, plus the corresponding associated missing transverse momentum. The missing transverse momentum vector, $\vec{p}_{\mathrm{T}}^{\,\mathrm{miss}}$, is defined as the negative vector sum of the momenta of all reconstructed PF candidates projected onto the plane perpendicular to the proton beams. Its magnitude is referred to as $p_{\mathrm{T}}^{\mathrm{miss}}$. Events with possible contributions from beam halo processes or anomalous noise in the calorimeters can have large values of $p_{\mathrm{T}}^{\mathrm{miss}}$ and are rejected using dedicated filters [64].

Electron candidates are reconstructed starting from a cluster of energy deposits in the ECAL. The cluster is then matched to a reconstructed track. The electron selection is based on the shower shape, the ratio of energy measured in the HCAL to that measured in the ECAL, track-cluster matching, and consistency between the cluster energy and the track momentum [65]. Muon candidates are reconstructed by performing a global fit that requires consistent hit patterns in the tracker and the muon system [66]. Photon candidates are reconstructed from a cluster of energy deposits in the ECAL, and they are required to pass criteria based on the shower shape and the ratio of energy measured in the HCAL to that measured in the ECAL [65]. Hadronically decaying tau lepton candidates (τ_{h}) are reconstructed from PF candidates with the "hadron-plus-strips" algorithm [67]. Electron, muon, photon, and τ_{h} candidates are required to be isolated from other particles, and electron, muon, and τ_{h} candidates must satisfy requirements on the transverse and longitudinal impact parameters relative to the primary vertex.

PF candidates are clustered to form jets using the anti-k_{T} clustering algorithm [62] with a distance parameter of 0.4, as implemented in the FastJet package [63]. Identification

JHEP03(2018)160

of jets originating from b quarks (b jets) is performed with either the combined secondary vertex (CSVv2) algorithm [68] or the DeepCSV algorithm [69]. Data events are selected using a variety of triggers requiring the presence of electrons, muons, photons, jets, or $p_{\mathrm{T}}^{\mathrm{miss}}$, depending on the final state targeted in each analysis.

Monte Carlo (MC) simulated samples are used in the various searches to estimate the background from some SM processes, to assess systematic uncertainties in prediction methods that rely on data, and to calculate the selection efficiency for signal models. Most SM background samples are produced with the MadGraph5_aMC@NLO v2.2.2 or v2.3.3 generator [70] at leading order (LO) or NLO accuracy in perturbative QCD, including up to four additional partons in the matrix element calculations, depending on the process and calculation order. Other samples are produced with the POWHEG v2 [71, 72] generator without additional partons in the matrix element calculations. Standard model WZ production in particular is modeled with MadGraph5_aMC@NLO v2.2.2 at NLO precision for the search described in section 6, which requires a precise description of initial-state radiation (ISR). In other cases, POWHEG v2 is used. The NNPDF3.0 LO or NLO [73] parton distribution functions (PDFs) are used in the event generation. Parton showering and fragmentation in all of these samples are performed using the PYTHIA v8.212 [74] generator and the CUETP8M1 tune [75]. A double counting of the partons generated with MadGraph5_aMC@NLO and those with PYTHIA is removed using the MLM [76] and the FxFx [77] matching schemes, in the LO and NLO samples, respectively. Cross section calculations at NLO or next-to-NLO [70, 78–82] are used to normalize the simulated background samples.

Signal samples are generated with MadGraph5_aMC@NLO at LO precision, including up to two additional partons in the matrix element calculations. Cross section calculations to NLO plus NLL accuracy [55, 56, 83] are used to normalize the signal samples. For these samples we improve on the modeling of ISR, which affects the total transverse momentum of the system of SUSY particles ($p_{\mathrm{T}}^{\mathrm{ISR}}$), by reweighting the $p_{\mathrm{T}}^{\mathrm{ISR}}$ distribution in these events. This reweighting procedure is based on experimental studies of the p_{T} of Z bosons [84]. The reweighting factors range between 1.18 (at $p_{\mathrm{T}}^{\mathrm{ISR}} = 125\,\mathrm{GeV}$) and 0.78 (for $p_{\mathrm{T}}^{\mathrm{ISR}} > 600\,\mathrm{GeV}$). We take the deviation from 1.0 as the systematic uncertainty in the reweighting procedure.

For both signal and background events, additional simultaneous proton-proton interactions (pileup) are generated with PYTHIA and superimposed on the hard collisions. The response of the CMS detector for SM background samples is simulated using a Geant4-based model [85], while that for new physics signals is performed using the CMS fast simulation package [86]. All simulated events are processed with the same chain of reconstruction programs as used for collision data. Corrections are applied to simulated samples to account for differences between the trigger, b tagging, and lepton and photon selection efficiencies measured in data and the Geant4 simulation. Additional differences arising from the fast simulation modeling of selection efficiencies, as well as from the modeling of $p_{\mathrm{T}}^{\mathrm{miss}}$, are corrected in the fast simulation and included in the systematic uncertainties considered.

JHEP03(2018)160

Search	Signal topology WZ	WH	ZZ	ZH	HH
1ℓ $2b$		✓			
$4b$					✓
2ℓ on-Z	✓		✓	✓	
2ℓ soft	✓				
$\geq 3\ell$	✓	✓	✓	✓	✓
$H(\gamma\gamma)$		✓		✓	✓

Table 1. Summary of all experimental searches considered in the combination (rows), and the signal topologies for which each search is used in the combined results (columns). The searches are described in sections 5.1 through 5.6 and section 6. The $\geq 3\ell$ search described in section 5.5 is used for all signal topologies except for WZ, where the reoptimized search strategy from section 6 is employed instead.

5 Individual searches

The experimental searches included in the combination are briefly described here. Table 1 lists which searches are used to place exclusion limits for each of the topologies introduced in section 2. The selections for all searches were checked to be mutually exclusive, such that no events fulfill the signal region requirements for more than one search. No significant deviations from the SM predictions were observed in any of these searches.

5.1 Search for one lepton, two b jets, and p_T^{miss}

The "1ℓ $2b$" search [43], targeting the WH topology, selects events with exactly one charged lepton (e or μ), exactly two b jets, and large p_T^{miss}. The invariant mass of the two b jets is required to be consistent with the mass of the H boson. Kinematic variables are used to suppress backgrounds, which predominantly come from dileptonic decays in $t\bar{t}$ production. Two exclusive signal regions are defined based on p_T^{miss}: $125 \leq p_T^{miss} < 200$ GeV and $p_T^{miss} \geq 200$ GeV. The SM backgrounds are predicted using MC simulation, with the predictions validated in data control regions distinct from the signal region.

5.2 Search for four b jets and p_T^{miss}

The "$4b$" search [41], targeting the HH topology, selects events with exactly four or five jets, with at least two of them identified as b jets, large p_T^{miss}, and no charged leptons. In each event, the four jets with the highest b tagging discriminator scores are considered to form dijet H candidates. There are three possible groupings to make two pairs of jets. The grouping is selected to minimize the difference between the invariant masses of the two dijet pairs, and the difference in masses is required to be less than 40 GeV. The average invariant mass of the two pairs is then required to be consistent with the mass of the H boson. Exclusive signal regions are defined based on the number of b jets (three or at least four) and multiple bins in p_T^{miss}. The primary background to this search comes from semileptonic decays in $t\bar{t}$ production, with smaller contributions from W or Z production in association with jets and from QCD multijet production. The backgrounds are predicted using data control samples that require either exactly two b jets or an average dijet invariant mass inconsistent with the H boson.

5.3 Search for two leptons consistent with a Z boson, jets, and p_T^{miss}

The "2ℓ on-Z" search [42], targeting the WZ, ZZ, and ZH topologies, selects events with exactly two opposite-sign, same-flavor (OSSF) leptons (e^+e^- or $\mu^+\mu^-$) consistent with the Z boson mass, at least two jets, and large p_T^{miss}. In the signal region targeting the WZ and ZZ topologies, two jets are required to have an invariant mass less than 110 GeV to be compatible with the W and Z boson masses, and events with b jets are rejected. To target the ZH topology, events are required to have two b jets with an invariant mass less than 150 GeV to be compatible with the H boson mass. Signal regions are defined with multiple exclusive bins in p_T^{miss}. The backgrounds fall into three categories. First, flavor symmetric backgrounds, such as $t\bar{t}$ production, yield $e^\pm\mu^\mp$ events at the same rate as e^+e^- and $\mu^+\mu^-$ events combined, and they are predicted from a data control sample of $e^\pm\mu^\mp$ events. Second, events with a Z boson and mismeasured jets give instrumental p_T^{miss}, and they are predicted from a data control sample of γ+jets events. Third, events with a Z boson and at least one prompt neutrino, arising from processes such as WZ, ZZ, and $t\bar{t}Z$ production, are estimated using simulation.

5.4 Search for two soft leptons and p_T^{miss}

The "2ℓ soft" search [39] selects events with exactly two low-p_T leptons (e^+e^- or $\mu^+\mu^-$ in the relevant selections), jets, and large p_T^{miss}. It targets the WZ topology where the mass difference between $\widetilde{\chi}_2^0$ and $\widetilde{\chi}_1^0$ is small such that the W and Z bosons are off-shell, and the observable decay products have low momentum. The leptons are required to satisfy $5 < p_T < 30$ GeV and have an invariant mass in the range $4 < m_{\ell\ell} < 50$ GeV, strongly suppressing SM backgrounds while retaining good acceptance for compressed signal scenarios. Additional kinematic requirements are applied to further reduce backgrounds, and the relevant signal regions are binned in $m_{\ell\ell}$ and p_T^{miss}. The largest backgrounds arise from Z/γ^* and $t\bar{t}$ production, as well as misidentification of nonprompt leptons. The first two are predicted from simulation with constraints from data control regions, while the latter is predicted entirely using data.

5.5 Search for three or more leptons, and p_T^{miss}

The "$\geq$3ℓ" search [38] selects events with three or more leptons (e, μ, and up to two τ_h) and large p_T^{miss}. Several exclusive categories are defined based on the number of leptons, lepton flavor and charge, the presence of an OSSF pair, and kinematic variables such as the invariant mass of the OSSF pair and p_T^{miss}. Events with a b jet are rejected to reduce the background from $t\bar{t}$ production. The various categories are designed to give this search sensitivity for a wide range of new physics models, including all of the topologies introduced in section 2. The best performance is seen in the WZ and ZZ models, while the lower branching fraction of the H boson to leptons reduces the sensitivity to other models. The SM backgrounds in this search vary across the categories, and the most important for the relevant regions in these interpretations are SM WZ and ZZ production, and events with misidentified nonprompt leptons. The former are predicted using simulation, which in case of WZ is validated in a set of dedicated control regions, while the latter are predicted entirely from data.

JHEP03(2018)160

A further optimization of this analysis has been performed for the WZ topology in the case where the difference in the masses of $\widetilde{\chi}_2^0$ and $\widetilde{\chi}_1^0$ is equal to the Z boson mass, focusing on a category selecting events with three light-flavor leptons (e, μ). This update is presented in section 6.

5.6 Search for a H boson decaying to diphotons and $p_{\mathrm{T}}^{\mathrm{miss}}$

The "H($\gamma\gamma$)" search [40] selects events with two photons consistent with the H boson mass, along with jets and large $p_{\mathrm{T}}^{\mathrm{miss}}$. Events are categorized based on the p_{T} of the diphoton system, the expected resolution on the diphoton mass, the presence of two b jets compatible with the H or Z boson masses, and the razor kinematic variables [87, 88]. It exhibits sensitivity to the WH, ZH, and HH topologies. The background arises either from γ+jets or SM H boson production. The former is estimated using a fit to the diphoton mass spectrum in a wider range than the signal window, while the latter is predicted using simulation.

6 Search for three light leptons consistent with WZ production and $p_{\mathrm{T}}^{\mathrm{miss}}$

The multilepton search described in section 5.5 contains a category selecting events with three light-flavor leptons (e, μ), two of which must form an OSSF pair. This final state aims to provide sensitivity for a variety of SUSY models, including the WZ topology depicted in figure 1 (left). The dominant background in this search category is SM WZ production.

Exclusion limits on the WZ topology were placed in ref. [38], and the sensitivity was found to be significantly reduced for $m_{\widetilde{\chi}_2^0} - m_{\widetilde{\chi}_1^0} \approx m_{\mathrm{Z}}$, referred to here as the "WZ corridor." In this case, SUSY signal is kinematically similar to the SM background. We present here a further optimization of the search for the WZ topology designed to target this challenging region of phase space. The search methodology remains the same as in ref. [38], but the event categorization has been updated as described below.

We require events to have three light-flavor leptons with two forming an OSSF pair. Events are categorized using the following kinematic variables: $p_{\mathrm{T}}^{\mathrm{miss}}$, the invariant mass $m_{\ell\ell}$ of the OSSF pair, and the transverse mass M_{T} of the third lepton computed with respect to $p_{\mathrm{T}}^{\mathrm{miss}}$. Three bins in $m_{\ell\ell}$ are defined to separate contributions from on- and off-shell Z boson decays, and three bins are defined in M_{T} to separate the SM W boson contribution.

To improve the separation between signal and background in the WZ corridor, we exploit ISR by further categorizing the events in H_{T}, the scalar p_{T} sum of the jets with $p_{\mathrm{T}} > 30\,\mathrm{GeV}$. Due to the presence of the $\widetilde{\chi}_1^0$ LSPs, signal model points in the WZ corridor will tend to have more events at high values of $p_{\mathrm{T}}^{\mathrm{miss}}$ and M_{T} than the SM background for the same value of H_{T}, with the effect becoming relevant at $m_{\widetilde{\chi}_1^0} \approx m_{\mathrm{Z}}$ and more pronounced at higher H_{T}. This is demonstrated in figure 4, which shows the expected distributions of $p_{\mathrm{T}}^{\mathrm{miss}}$ for background and two signal model points after requiring (left) $H_{\mathrm{T}} < 100\,\mathrm{GeV}$ and (right) $\geq 200\,\mathrm{GeV}$. The H_{T} categorization is applied in the regions $m_{\ell\ell} < 75\,\mathrm{GeV}$ and $75 \leq m_{\ell\ell} < 105\,\mathrm{GeV}$. The full set of search regions is summarized in table 2.

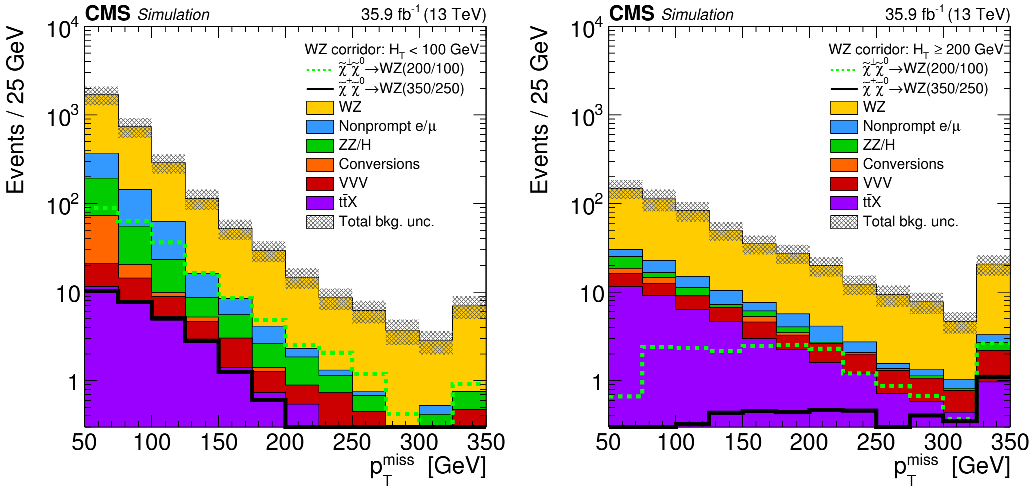

Figure 4. Distributions of $p_{\mathrm{T}}^{\mathrm{miss}}$ for two representative signal points in the WZ corridor as well as the expected SM background for $H_{\mathrm{T}} < 100$ (left) and $\geq 200\,\mathrm{GeV}$ (right). The mass values for the signal points are given as $(m_{\tilde{\chi}_2^0}/m_{\tilde{\chi}_1^0})$ in GeV. For larger values of H_{T}, the shape difference between signal and background becomes more pronounced due to the presence of $\tilde{\chi}_1^0$ LSPs with large Lorentz boost.

The dominant background in this search is SM WZ production, which provides a signature very similar to the signal process in the form of three isolated leptons and substantial $p_{\mathrm{T}}^{\mathrm{miss}}$ due to the neutrino from the W boson decay. This background is estimated from simulation, while two control regions are used to assess the overall normalization and to validate the modeling of events at large values of $p_{\mathrm{T}}^{\mathrm{miss}}$, M_{T}, or both. Further backgrounds arise from misidentification of nonprompt leptons from processes like $\mathrm{t\bar{t}}$ production, external and internal photon conversions, and rare SM processes such as triboson production, $\mathrm{t\bar{t}W}$, and $\mathrm{t\bar{t}Z}$. The contribution of the nonprompt lepton background is predicted using the “tight-to-loose” ratio method [89], which relies entirely on data. External and internal photon conversions as well as rare SM processes are predicted from simulation, and a dedicated data control region is used to constrain the normalization of the conversion background.

The SM WZ background normalization is constrained in a data control region requiring $75 \leq m_{\ell\ell} < 105\,\mathrm{GeV}$, $M_{\mathrm{T}} < 100\,\mathrm{GeV}$, $35 < p_{\mathrm{T}}^{\mathrm{miss}} < 100\,\mathrm{GeV}$, and $H_{\mathrm{T}} < 100\,\mathrm{GeV}$. The fraction of selected background events arising from SM WZ production in this region is approximately 86%. The validation of the $p_{\mathrm{T}}^{\mathrm{miss}}$ and M_{T} shape modeling is done using a data control sample enriched in Wγ events, with the remainder of events coming mainly from W+jets production. A photon with $p_{\mathrm{T}} > 40\,\mathrm{GeV}$ is required together with a lepton and $p_{\mathrm{T}}^{\mathrm{miss}} \geq 50\,\mathrm{GeV}$, corresponding to a leptonic W boson decay. The minimum photon p_{T} threshold ensures that the photon does not arise from final-state radiation. The motivation behind this selection is that the W boson M_{T} distribution in both Wγ and W+jets events is found to be consistent with that of SM WZ production. A systematic uncertainty is assigned to the signal region bins with high M_{T} and $p_{\mathrm{T}}^{\mathrm{miss}}$ based on the statistical precision of this control region.

JHEP03(2018)160

<table>
<tr><th>$m_{\ell\ell}$ (GeV)</th><th>M_{T} (GeV)</th><th>$p_{\mathrm{T}}^{\mathrm{miss}}$ (GeV)</th><th>$H_{\mathrm{T}} < 100\,\mathrm{GeV}$</th><th>$100 \leq H_{\mathrm{T}} < 200\,\mathrm{GeV}$</th><th>$H_{\mathrm{T}} \geq 200\,\mathrm{GeV}$</th></tr>
<tr><td rowspan="11">0–75</td><td rowspan="4">0–100</td><td>50–100</td><td colspan="2">SR 01</td><td rowspan="4">SR 12</td></tr>
<tr><td>100–150</td><td colspan="2">SR 02</td></tr>
<tr><td>150–200</td><td colspan="2">SR 03</td></tr>
<tr><td>≥200</td><td colspan="2">SR 04</td></tr>
<tr><td rowspan="3">100–160</td><td>50–100</td><td colspan="2">SR 05</td><td rowspan="3">SR 13</td></tr>
<tr><td>100–150</td><td colspan="2">SR 06</td></tr>
<tr><td>≥150</td><td colspan="2">SR 07</td></tr>
<tr><td rowspan="4">≥160</td><td>50–100</td><td colspan="2">SR 08</td><td rowspan="4">SR 14</td></tr>
<tr><td>100–150</td><td colspan="2">SR 09</td></tr>
<tr><td>150–200</td><td colspan="2">SR 10</td></tr>
<tr><td>≥200</td><td colspan="2">SR 11</td></tr>
<tr><td rowspan="18">75–105</td><td rowspan="6">0–100</td><td>50–100</td><td>(WZ CR)</td><td>SR 27</td><td rowspan="2">SR 40</td></tr>
<tr><td>100–150</td><td>SR 15</td><td>SR 28</td></tr>
<tr><td>150–200</td><td>SR 16</td><td>SR 29</td><td rowspan="2">SR 41</td></tr>
<tr><td>200–250</td><td>SR 17</td><td>SR 30</td></tr>
<tr><td>250–350</td><td rowspan="2">SR 18</td><td rowspan="2">SR 31</td><td>SR 42</td></tr>
<tr><td>≥350</td><td>SR 43</td></tr>
<tr><td rowspan="6">100–160</td><td>50–100</td><td>SR 19</td><td>SR 32</td><td>SR 44</td></tr>
<tr><td>100–150</td><td>SR 20</td><td>SR 33</td><td>SR 45</td></tr>
<tr><td>150–200</td><td>SR 21</td><td>SR 34</td><td>SR 46</td></tr>
<tr><td>200–250</td><td rowspan="3">SR 22</td><td rowspan="3">SR 35</td><td>SR 47</td></tr>
<tr><td>250–300</td><td>SR 48</td></tr>
<tr><td>≥300</td><td>SR 49</td></tr>
<tr><td rowspan="6">≥160</td><td>50–100</td><td>SR 23</td><td>SR 36</td><td>SR 50</td></tr>
<tr><td>100–150</td><td>SR 24</td><td>SR 37</td><td>SR 51</td></tr>
<tr><td>150–200</td><td>SR 25</td><td>SR 38</td><td>SR 52</td></tr>
<tr><td>200–250</td><td rowspan="3">SR 26</td><td rowspan="3">SR 39</td><td>SR 53</td></tr>
<tr><td>250–300</td><td>SR 54</td></tr>
<tr><td>≥300</td><td>SR 55</td></tr>
<tr><td rowspan="3">≥105</td><td>0–100</td><td>≥50</td><td colspan="3">SR 56</td></tr>
<tr><td>100–160</td><td>≥50</td><td colspan="3">SR 57</td></tr>
<tr><td>≥160</td><td>≥50</td><td colspan="3">SR 58</td></tr>
</table>

Table 2. Definition of the search regions (SRs) optimized for the WZ corridor in the WZ signal topology. Events must have three leptons (e, μ) forming at least one OSSF pair and they are categorized in $m_{\ell\ell}$, M_{T}, $p_{\mathrm{T}}^{\mathrm{miss}}$ and H_{T}. Where ranges of values are given, the lower bound is inclusive while the upper bound is exclusive, e.g., $75 \leq m_{\ell\ell} < 105\,\mathrm{GeV}$.

Distributions of key kinematic observables for the events entering the search regions are shown in figure 5 with two representative signal mass points included. The data agree with the prediction within systematic uncertainties, which are dominated at high M_{T} and $p_{\mathrm{T}}^{\mathrm{miss}}$ by the WZ control region statistical precision as described above. This uncertainty is taken as correlated across signal region bins. The comparison between expected and observed yields in the search regions is shown in figure 6 and table 3. No significant deviations from the SM expectations are observed. The predicted background yields and uncertainties presented in this section are used as inputs to the likelihood fit for interpretation, described in section 7. The interpretation of the results in the WZ topology at 95% confidence level (CL) is presented in figure 7. Compared to ref. [38], the expected lower mass limit in the WZ corridor has improved from around $(m_{\tilde{\chi}_2^0}, m_{\tilde{\chi}_1^0}) = (200, 100)$ to around $(225, 125)\,\mathrm{GeV}$, while the observed limit has improved by around 60 GeV in both mass values. The expected

JHEP03(2018)160

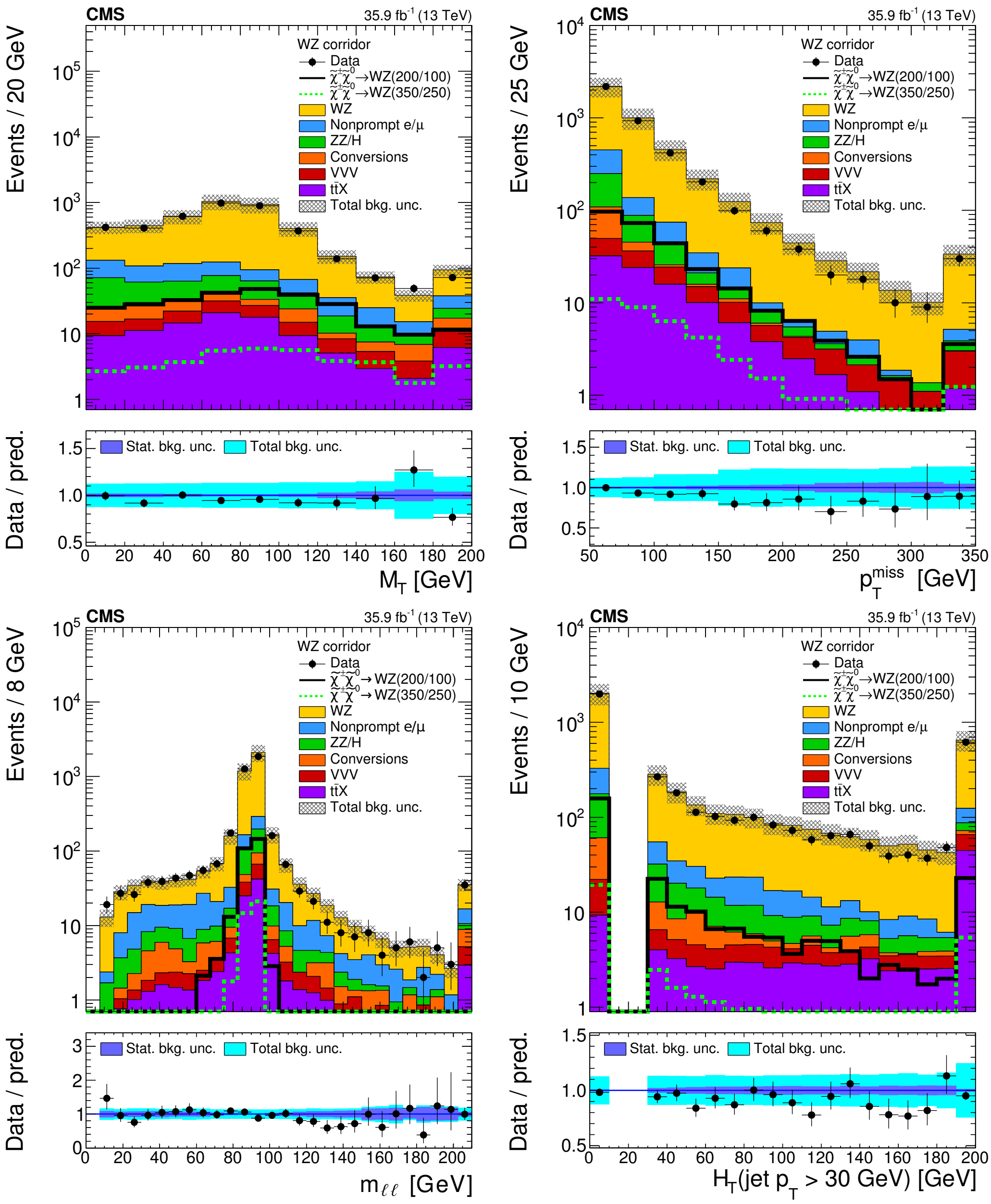

Figure 5. Distributions of the transverse mass of the third lepton with respect to $p_{\mathrm{T}}^{\mathrm{miss}}$ (upper left), the $p_{\mathrm{T}}^{\mathrm{miss}}$ (upper right), the $m_{\ell\ell}$ of the OSSF pair (lower left), and the H_{T} (lower right). Distributions for two signal mass points in the WZ corridor are overlaid for illustration. The mass values for the signal points are given as $(m_{\widetilde{\chi}_2^0}/m_{\widetilde{\chi}_1^0})$ in GeV. The bottom panel shows the ratio of observed data to predicted yields. The dark purple band shows the statistical uncertainty in the background prediction, while the light blue band shows the total uncertainty.

limit contour for signal points with $m_{\widetilde{\chi}_2^0} - m_{\widetilde{\chi}_1^0} > m_{\mathrm{Z}}$ has also improved by as much as 25 GeV due to the new selections. The upper limit on the $\widetilde{\chi}_1^{\pm}\widetilde{\chi}_2^0$ production cross section has improved by a factor of 2.

The event selections listed in table 2 are used to replace the selections for category A

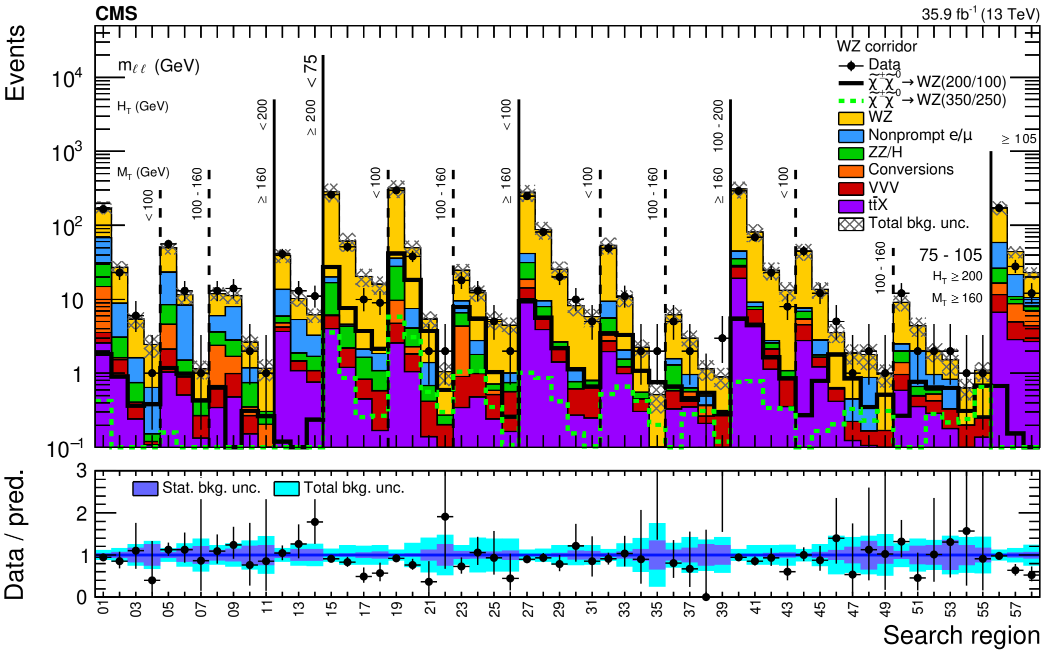

Figure 6. Expected and observed yield comparison in the search regions. Two example signal mass points along the WZ corridor are overlaid for illustration. The mass values for the signal points are given as $(m_{\widetilde{\chi}_2^0}/m_{\widetilde{\chi}_1^0})$ in GeV. The bottom panel shows the ratio of observed data to predicted yields. The dark purple band shows the statistical uncertainty in the background prediction, while the light blue band shows the total uncertainty.

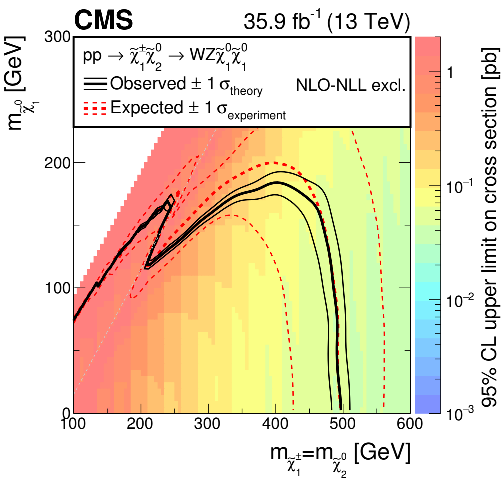

Figure 7. The 95% confidence level upper limit on the production cross section in the plane of $m_{\widetilde{\chi}_1^\pm}$ and $m_{\widetilde{\chi}_1^0}$ for the model of $\widetilde{\chi}_1^\pm\widetilde{\chi}_2^0$ production with the WZ topology, using only the search requiring three or more leptons as described in section 6. The thick solid black (dashed red) curve represents the observed (expected) exclusion contour assuming the theory cross sections. The area below each curve is the excluded region. The thin dashed red lines indicate the $\pm 1\sigma_{\text{experiment}}$ uncertainty. The thin black lines show the effect of the theoretical uncertainties ($\pm 1\sigma_{\text{theory}}$) on the signal cross section. The color scale shows the observed limit at 95% CL on the signal production cross section.

<table>
<tr><th>$m_{\ell\ell}$ (GeV)</th><th>M_{T} (GeV)</th><th>$p_{\mathrm{T}}^{\mathrm{miss}}$ (GeV)</th><th colspan="2">$H_{\mathrm{T}} < 100\,\mathrm{GeV}$</th><th colspan="2">$100 \leq H_{\mathrm{T}} < 200\,\mathrm{GeV}$</th><th colspan="2">$H_{\mathrm{T}} \geq 200\,\mathrm{GeV}$</th></tr>
<tr><td rowspan="11">0–75</td><td rowspan="4">0–100</td><td>50–100</td><td colspan="2">175 ± 20</td><td colspan="2">166</td><td rowspan="4">39 ± 6</td><td rowspan="4">41</td></tr>
<tr><td>100–150</td><td colspan="2">27 ± 4</td><td colspan="2">23</td></tr>
<tr><td>150–200</td><td colspan="2">5 ± 1</td><td colspan="2">6</td></tr>
<tr><td>≥200</td><td colspan="2">2.5 ± 0.8</td><td colspan="2">1</td></tr>
<tr><td rowspan="3">100–160</td><td>50–100</td><td colspan="2">50 ± 8</td><td colspan="2">56</td><td rowspan="3">10 ± 3</td><td rowspan="3">13</td></tr>
<tr><td>100–150</td><td colspan="2">12 ± 3</td><td colspan="2">13</td></tr>
<tr><td>≥150</td><td colspan="2">1.2 ± 0.4</td><td colspan="2">1</td></tr>
<tr><td rowspan="4">≥160</td><td>50–100</td><td colspan="2">12 ± 2</td><td colspan="2">13</td><td rowspan="4">6 ± 2</td><td rowspan="4">11</td></tr>
<tr><td>100–150</td><td colspan="2">11 ± 3</td><td colspan="2">14</td></tr>
<tr><td>150–200</td><td colspan="2">2.6 ± 0.9</td><td colspan="2">2</td></tr>
<tr><td>≥200</td><td colspan="2">1.2 ± 0.5</td><td colspan="2">1</td></tr>
<tr><td rowspan="18">75–105</td><td rowspan="6">0–100</td><td>50–100</td><td colspan="2">(WZ CR)</td><td>279 ± 34</td><td>250</td><td rowspan="2">310 ± 40</td><td rowspan="2">292</td></tr>
<tr><td>100–150</td><td>286 ± 44</td><td>260</td><td>87 ± 13</td><td>81</td></tr>
<tr><td>150–200</td><td>62 ± 14</td><td>51</td><td>26 ± 6</td><td>20</td><td rowspan="2">81 ± 18</td><td rowspan="2">69</td></tr>
<tr><td>200–250</td><td>20 ± 5</td><td>10</td><td>8 ± 2</td><td>10</td></tr>
<tr><td>250–350</td><td rowspan="2">16 ± 4</td><td rowspan="2">9</td><td rowspan="2">6 ± 1</td><td rowspan="2">5</td><td>25 ± 6</td><td>23</td></tr>
<tr><td>≥350</td><td>13 ± 3</td><td>8</td></tr>
<tr><td rowspan="6">100–160</td><td>50–100</td><td>321 ± 42</td><td>297</td><td>54 ± 8</td><td>49</td><td>45 ± 6</td><td>45</td></tr>
<tr><td>100–150</td><td>50 ± 14</td><td>38</td><td>11 ± 3</td><td>11</td><td>14 ± 3</td><td>12</td></tr>
<tr><td>150–200</td><td>5 ± 2</td><td>2</td><td>2.2 ± 0.9</td><td>2</td><td>4 ± 2</td><td>5</td></tr>
<tr><td>200–250</td><td rowspan="3">1.1 ± 0.5</td><td rowspan="3">2</td><td rowspan="3">0.5 ± 0.4</td><td rowspan="3">2</td><td>1.9 ± 0.8</td><td>1</td></tr>
<tr><td>250–300</td><td>1.8 ± 0.8</td><td>2</td></tr>
<tr><td>≥300</td><td>1.0 ± 0.5</td><td>1</td></tr>
<tr><td rowspan="6">≥160</td><td>50–100</td><td>25 ± 6</td><td>18</td><td>6 ± 2</td><td>5</td><td>9 ± 3</td><td>12</td></tr>
<tr><td>100–150</td><td>12 ± 5</td><td>13</td><td>3.0 ± 1.3</td><td>2</td><td>4 ± 2</td><td>2</td></tr>
<tr><td>150–200</td><td>5 ± 2</td><td>5</td><td>1.1 ± 0.4</td><td>0</td><td>2.0 ± 0.7</td><td>2</td></tr>
<tr><td>200–250</td><td rowspan="3">4 ± 2</td><td rowspan="3">2</td><td rowspan="3">0.9 ± 0.4</td><td rowspan="3">3</td><td>1.5 ± 0.7</td><td>2</td></tr>
<tr><td>250–300</td><td>0.6 ± 0.3</td><td>1</td></tr>
<tr><td>≥300</td><td>1.1 ± 0.5</td><td>1</td></tr>
<tr><td rowspan="3">≥105</td><td>0–100</td><td>≥50</td><td colspan="3">173 ± 21</td><td colspan="3">170</td></tr>
<tr><td>100–160</td><td>≥50</td><td colspan="3">44 ± 7</td><td colspan="3">28</td></tr>
<tr><td>≥160</td><td>≥50</td><td colspan="3">23 ± 6</td><td colspan="3">12</td></tr>
</table>

Table 3. Expected and observed event yields in the search regions. For each bin, the first number corresponds to the expected yield and its total uncertainty while the second number gives the observation. Where ranges of values are given for the selections, the lower bound is inclusive while the upper bound is exclusive, e.g., $75 \leq m_{\ell\ell} < 105\,\mathrm{GeV}$.

in ref. [38] in the combination below with other analyses, when interpreting results in the models with either 100% or 50% branching fraction to the SUSY WZ topology. In this case, the systematic uncertainties in the background prediction are treated as being fully correlated with the other categories from ref. [38].

7 Interpretation

The results of the searches described in sections 5 and 6 are interpreted using the simplified models introduced in section 2. Cross section limits as a function of the SUSY particle masses are set using a modified frequentist approach, employing the $\mathrm{CL_s}$ criterion and an asymptotic formulation [90–93]. The uncertainties in the signal efficiency and acceptance and in the background predictions are incorporated as nuisance parameters. The observed data yields in control regions are typically incorporated either by a simultaneous maximum likelihood fit of the signal and control regions or through parameterization using the gamma function. Other nuisance parameters are implemented using lognormal functions, whose widths reflect the size of the systematic uncertainty, or as alternate shapes of the relevant distributions. Within each signal model, the experimental and theoretical uncertainties affecting the signal prediction are treated as fully correlated for all analyses. The dominant uncertainties in the background predictions are not correlated among analyses as they tend to be either statistical in nature, arising from independent control regions, or uncertainties in the prediction methods, which are unique to each analysis. For each signal topology, the analyses with a check mark in table 1 are combined to place exclusion limits.

The following sources of uncertainty in the signal acceptance and efficiency are assumed to be fully correlated among analyses: determination of the integrated luminosity, lepton identification and isolation efficiency, lepton efficiency modeling in fast simulation, b tagging efficiency, jet energy scale, modeling of $p_{\mathrm{T}}^{\mathrm{miss}}$ in fast simulation, modeling of ISR, simulation of pileup, and variations of the generator factorization and renormalization scales. Variations in the PDF set used are found to primarily affect the signal acceptance by changing the p_{T} distribution of the initially-produced sparticle pair, $\widetilde{\chi}_1^{\pm}\widetilde{\chi}_2^0$ or $\widetilde{\chi}_1^0\widetilde{\chi}_1^0$. This is already incorporated in the empirical uncertainty in the modeling of ISR as described in section 4, and we therefore do not apply a dedicated uncertainty in signal acceptance from PDF variations. All analyses also include the statistical uncertainty of the simulated signal samples, which is taken as being uncorrelated in every bin, and the uncertainty in the modeling of the trigger efficiency, which is also taken as uncorrelated given the different trigger requirements applied in each analysis. Some analyses have additional uncertainties beyond these, such as the uncertainty in the modeling of the diphoton mass resolution for the $\mathrm{H}(\gamma\gamma)$ analysis, which are analysis-specific and treated as being uncorrelated.

For the models of $\widetilde{\chi}_1^{\pm}\widetilde{\chi}_2^0$ production, 95% confidence level exclusion limits are presented in the plane of $m_{\widetilde{\chi}_1^{\pm}}$ and $m_{\widetilde{\chi}_1^0}$. Figure 8 shows the exclusion limits for the combination of analyses for the WZ topology, the WH topology, and the mixed topology with 50% branching fraction to each of the WZ and WH channels. Figure 9 shows the analysis with the best expected limit for each point in the plane for the same topologies. The on-Z dilepton analysis generally gives the best sensitivity for large values of $\Delta m = m_{\widetilde{\chi}_2^0} - m_{\widetilde{\chi}_1^0}$. The search for three light-flavor leptons provides the best sensitivity at intermediate values of Δm, including the region where $\Delta m \approx m_{\mathrm{Z}}$, while the soft-dilepton analysis provides unique sensitivity to the smallest values of Δm. Figure 10 (left) shows the observed and expected limit contours for each of the individual analyses considered in the combination, and figure 10 (right) shows the results from the combination for all three topologies considered. For a massless LSP $\widetilde{\chi}_1^0$, the combined result gives an observed (expected) limit in $m_{\widetilde{\chi}_1^{\pm}}$ of about 650 (570) GeV for the WZ topology, 480 (455) GeV for the WH topology, and 535 (440) GeV for the mixed topology. The combination also excludes intermediate mass values that were not excluded by individual analyses, including $m_{\widetilde{\chi}_1^{\pm}}$ values between 180 and 240 GeV for a massless LSP in the WH topology.

For the models of $\widetilde{\chi}_1^0\widetilde{\chi}_1^0$ production, the exclusion limits are presented in the plane of $m_{\widetilde{\chi}_1^0}$ and the branching fraction $\mathcal{B}(\widetilde{\chi}_1^0 \to \mathrm{H}\widetilde{G})$. The decay $\widetilde{\chi}_1^0 \to \mathrm{Z}\widetilde{G}$ is assumed to make up the remainder of the branching fraction. Figure 11 shows the observed and expected limits

JHEP03(2018)160

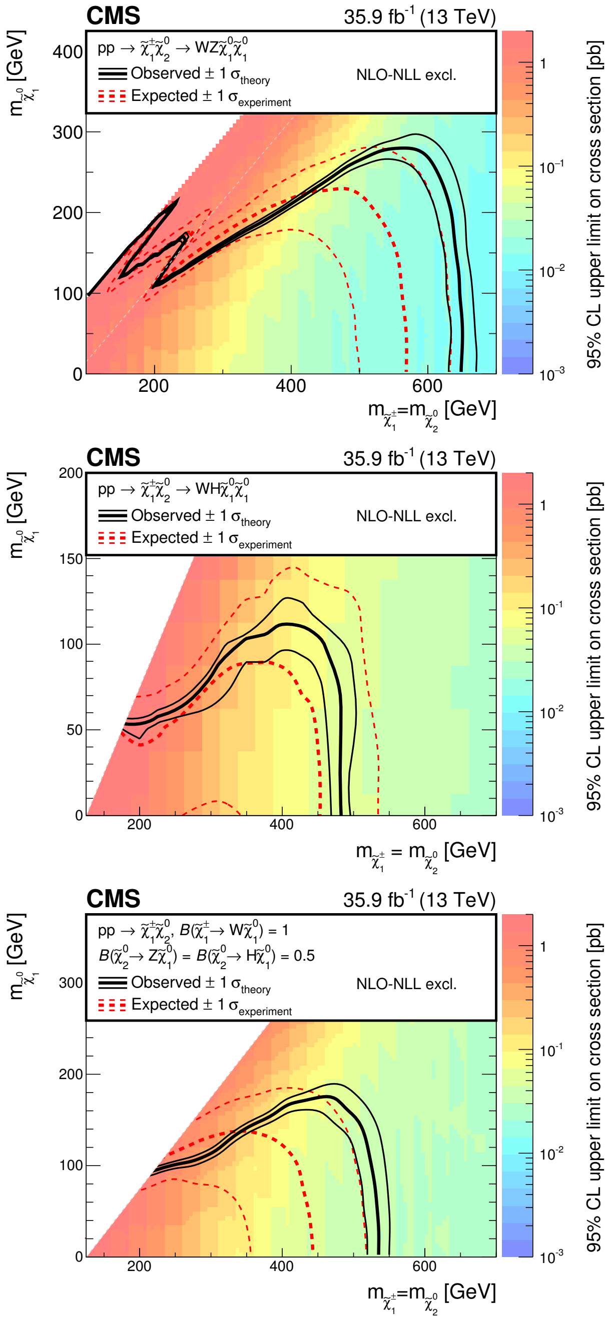

Figure 8. The 95% CL upper limits on the production cross sections in the plane of $m_{\widetilde{\chi}_1^\pm}$ and $m_{\widetilde{\chi}_1^0}$ for the models of $\widetilde{\chi}_1^\pm\widetilde{\chi}_2^0$ production with (upper) the WZ topology, (middle) the WH topology, or (lower) the mixed topology with 50% branching fraction to each of WZ and WH. The thick solid black (dashed red) curve represents the observed (expected) exclusion contour assuming the theory cross sections. The area below each curve is the excluded region. The thin dashed red lines indicate the $\pm 1\sigma_{\text{experiment}}$ uncertainty. The thin black lines show the effect of the theoretical uncertainties ($\pm 1\sigma_{\text{theory}}$) on the signal cross section. The color scale shows the observed limit at 95% CL on the signal production cross section.

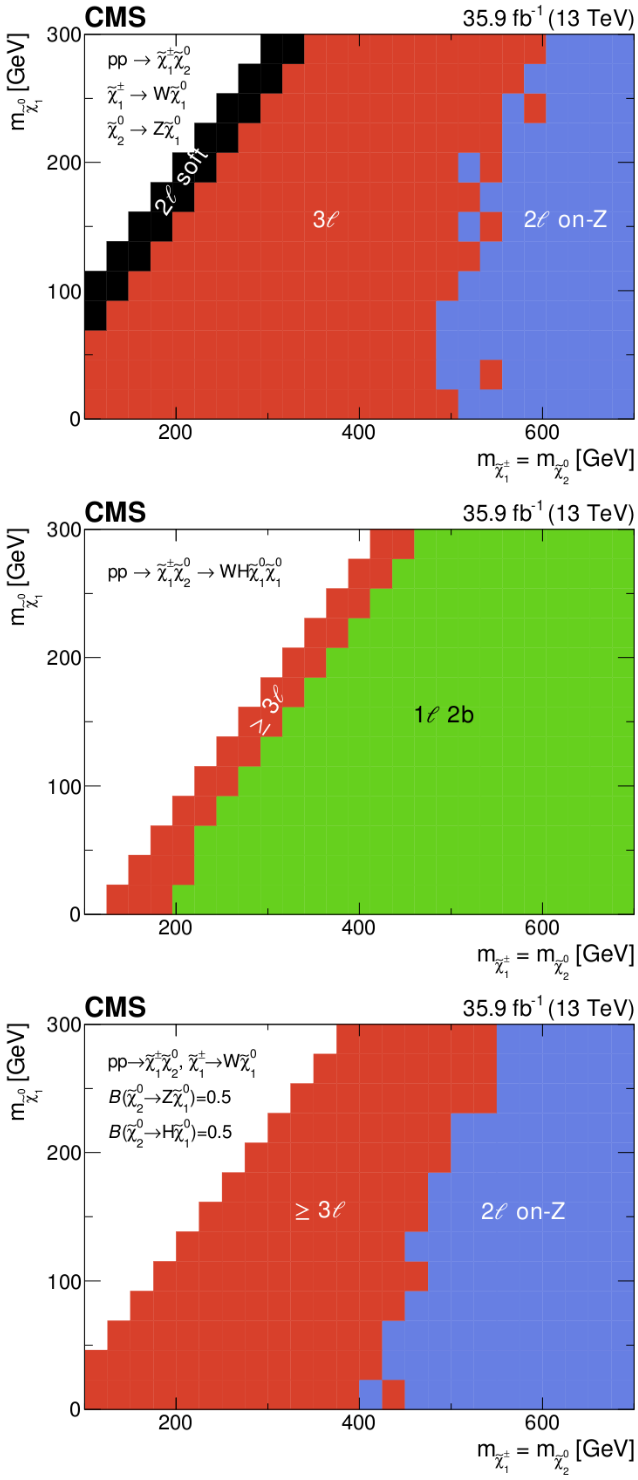

Figure 9. The analysis with the best expected exclusion limit at each point in the plane of $m_{\widetilde{\chi}_1^\pm}$ and $m_{\widetilde{\chi}_1^0}$ for the models of $\widetilde{\chi}_1^\pm \widetilde{\chi}_2^0$ production with (upper) the WZ topology, (middle) the WH topology, and (lower) the mixed topology 50% branching fraction to each of WZ and WH.

JHEP03(2018)160

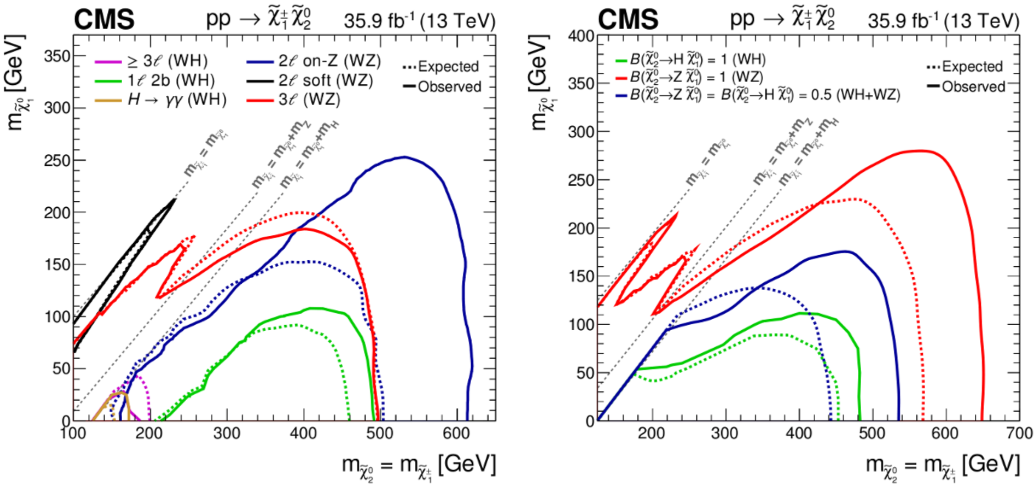

Figure 10. Exclusion contours at 95% CL in the plane of $m_{\tilde{\chi}_1^\pm}$ and $m_{\tilde{\chi}_1^0}$ for the models of $\tilde{\chi}_1^\pm \tilde{\chi}_2^0$ production (left) for the individual analyses and (right) for the combination of analyses. The decay modes assumed for each contour are given in the legends.

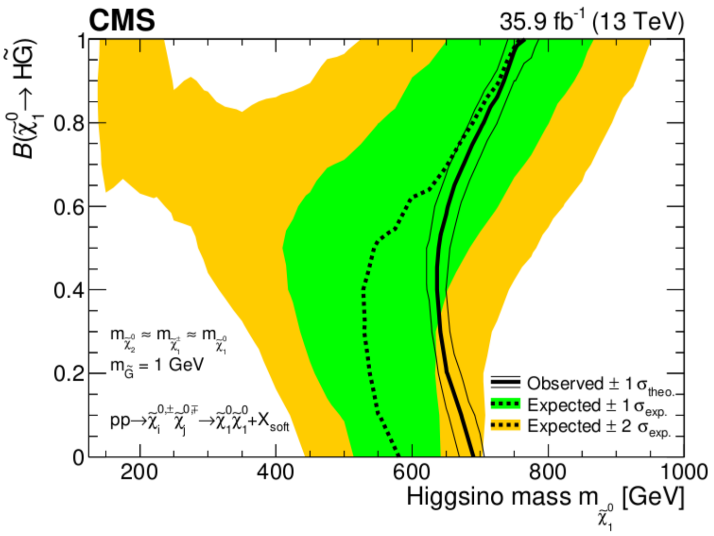

Figure 11. Combined exclusion contours at the 95% CL in the plane of $m_{\tilde{\chi}_1^0}$ and $\mathcal{B}(\tilde{\chi}_1^0 \to \mathrm{H}\tilde{G})$ for the model of $\tilde{\chi}_1^0 \tilde{\chi}_1^0$ production. The area to the left of or below the solid (dashed) black curve represents the observed (expected) exclusion region. The green and yellow bands indicate the ±1 and 2σ uncertainties in the expected limit. The thin black lines show the effect of the theoretical uncertainties ($\pm 1\sigma_{\text{theory}}$) on the signal cross section.

from the combination in this plane. The expected mass exclusion limit varies between about 550 and 750 GeV, being least stringent around $\mathcal{B}(\tilde{\chi}_1^0 \to \mathrm{H}\tilde{G}) = 0.4$. The observed limit ranges between about 650 and 750 GeV, allowing us to exclude masses below 650 GeV independent of this branching fraction.

Figure 12 shows the observed limits from each analysis separately compared with the combined result. Figure 13 shows the analysis with the best expected exclusion limit

JHEP03(2018)160

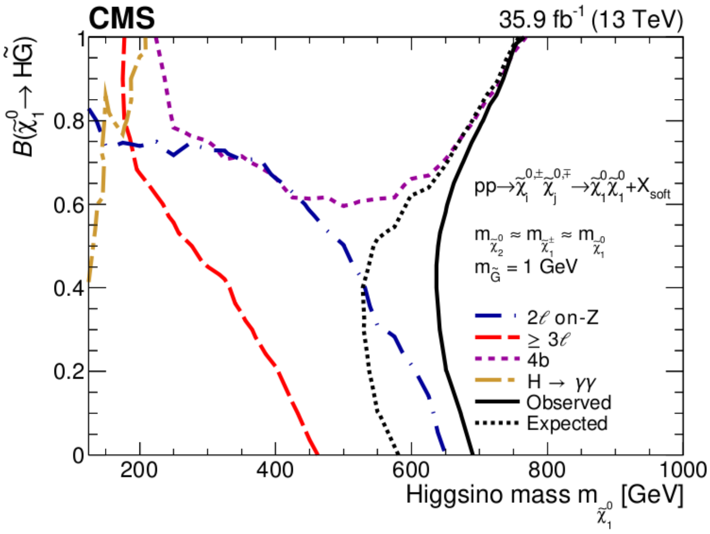

Figure 12. Observed exclusion contours at the 95% CL in the plane of $m_{\tilde{\chi}^0_1}$ and $\mathcal{B}(\tilde{\chi}^0_1 \to \mathrm{H}\widetilde{G})$ for the model of $\tilde{\chi}^0_1\tilde{\chi}^0_1$ production for each individual analysis compared with the combination. For the 4b contour, the region above is excluded, while for all others, the region to the left is excluded. The 4b search drives the exclusion at large values of $\mathcal{B}(\tilde{\chi}^0_1 \to \mathrm{H}\widetilde{G})$ while the on-Z dilepton and multilepton searches are competing at lower values of $\mathcal{B}(\tilde{\chi}^0_1 \to \mathrm{H}\widetilde{G})$.

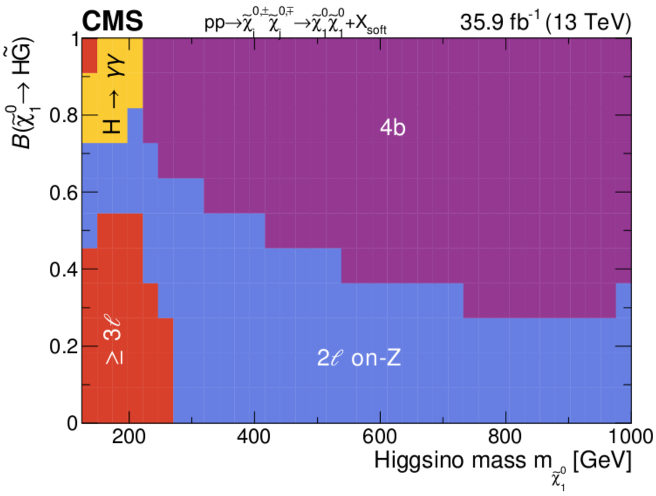

Figure 13. The analysis with the best expected exclusion limit at each point in the plane of $m_{\tilde{\chi}^0_1}$ and $\mathcal{B}(\tilde{\chi}^0_1 \to \mathrm{H}\widetilde{G})$ for the model of $\tilde{\chi}^0_1\tilde{\chi}^0_1$ production.

for each point in the same plane. At higher values of $m_{\tilde{\chi}^0_1}$, the searches for at least one hadronically decaying boson provide the best sensitivity, the 4b search when $\mathcal{B}(\tilde{\chi}^0_1 \to \mathrm{H}\widetilde{G})$ is large and the on-Z dilepton search when it is smaller. At lower values of $m_{\tilde{\chi}^0_1}$, below around 200 GeV, the H($\gamma\gamma$) analysis is most sensitive when $\mathcal{B}(\tilde{\chi}^0_1 \to \mathrm{H}\widetilde{G})$ is large, while the three or more lepton search is dominant when it is small. Figure 14 then shows the exclusion limits as a function of $m_{\tilde{\chi}^0_1}$ for three choices of $\mathcal{B}(\tilde{\chi}^0_1 \to \mathrm{H}\widetilde{G})$: 0%, yielding the ZZ topology; 100%, yielding the HH topology; and 50%, yielding a mix of events from the

JHEP03(2018)160

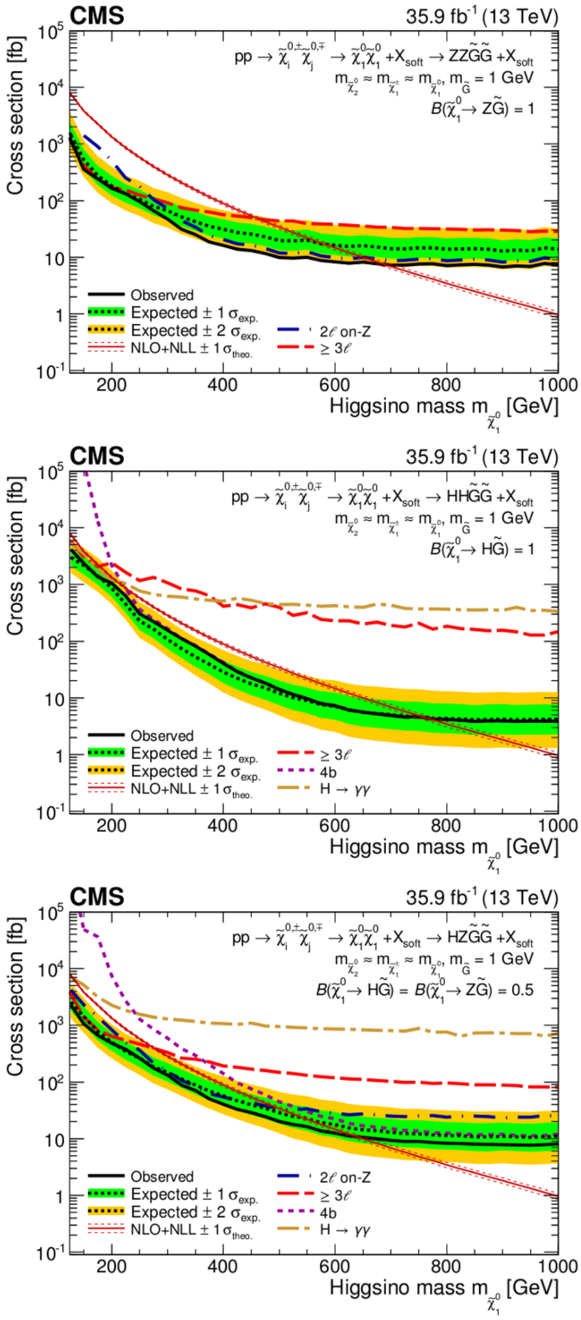

Figure 14. The 95% CL upper limits on the production cross sections as a function of $m_{\widetilde{\chi}^0_1}$ for the model of $\widetilde{\chi}^0_1\widetilde{\chi}^0_1$ production with three choices of $\mathcal{B}(\widetilde{\chi}^0_1 \to \mathrm{H}\widetilde{G})$: (upper) 0%, yielding the ZZ topology, (middle) 100%, yielding the HH topology, and (lower) 50%, yielding the ZH mixed topology. The solid black line represents the observed exclusion. The dashed black line represents the expected exclusion, while the green and yellow bands indicate the ± 1 and 2σ uncertainties in the expected limit. The red line shows the theoretical cross section with its uncertainty. The other lines in each plot show the observed exclusion for individual analyses.

JHEP03(2018)160

ZZ, HH, and ZH topologies.

8 Summary

A number of searches for the electroweak production of charginos and neutralinos predicted in supersymmetry (SUSY) have been performed in different final states. All searches considered here use proton-proton collision data at $\sqrt{s} = 13\,\text{TeV}$, recorded with the CMS detector at the LHC and corresponding to an integrated luminosity of $35.9\,\text{fb}^{-1}$. No significant deviations from the standard model expectations have been observed.

A targeted search requiring three or more charged leptons (electrons or muons) has been presented, focusing on chargino-neutralino production where the difference in mass between $\widetilde{\chi}^0_2$ and $\widetilde{\chi}^0_1$ is approximately equal to the mass of the Z boson, and no significant deviations from the standard model predictions are observed. This search is interpreted in a simplified model scenario of SUSY chargino-neutralino ($\widetilde{\chi}^{\pm}_1\widetilde{\chi}^0_2$) production with decays $\widetilde{\chi}^{\pm}_1 \to \mathrm{W}^{\pm}\widetilde{\chi}^0_1$ and $\widetilde{\chi}^0_2 \to \mathrm{Z}\widetilde{\chi}^0_1$, where $\widetilde{\chi}^0_1$ is the lightest SUSY particle (LSP). In the targeted phase space, the expected and observed 95% confidence level exclusion limits extend to 225 GeV in the mass of $\widetilde{\chi}^0_2$ and 125 GeV in the mass of $\widetilde{\chi}^0_1$, improving the observed limits from the previous publication by up to 60 GeV [38].

A statistical combination of several searches is performed and interpreted in the context of simplified models of either chargino-neutralino production, or neutralino pair production in a gauge-mediated SUSY breaking (GMSB) scenario. For a massless LSP $\widetilde{\chi}^0_1$ in the chargino-neutralino model, the combined result gives an observed (expected) limit in the $\widetilde{\chi}^{\pm}_1$ mass of about 650 (570) GeV for the WZ topology, 480 (455) GeV for the WH topology, and 535 (440) GeV for the mixed topology. Compared to the results of individual analyses, the combination improves the observed exclusion limit by up to 40 GeV in the masses of $\widetilde{\chi}^{\pm}_1$ and $\widetilde{\chi}^0_2$ in the chargino-neutralino model. The combination also excludes intermediate mass values that were not excluded by individual analyses, including $\widetilde{\chi}^{\pm}_1$ masses between 180 and 240 GeV in the WH topology. In the GMSB neutralino pair model, the combined result gives an observed (expected) limit in the $\widetilde{\chi}^0_1$ mass of 650–750 (550–750) GeV. The combined result improves the observed limit by up to 200 GeV in the mass of $\widetilde{\chi}^0_1$ in the GMSB neutralino pair model, depending on the branching fractions for the SUSY particle decays. These results represent the most stringent constraints to date for all models considered.

Acknowledgments

We congratulate our colleagues in the CERN accelerator departments for the excellent performance of the LHC and thank the technical and administrative staffs at CERN and at other CMS institutes for their contributions to the success of the CMS effort. In addition, we gratefully acknowledge the computing centers and personnel of the Worldwide LHC Computing Grid for delivering so effectively the computing infrastructure essential to our analyses. Finally, we acknowledge the enduring support for the construction and operation of the LHC and the CMS detector provided by the following funding agencies: BMWFW and FWF (Austria); FNRS and FWO (Belgium); CNPq, CAPES, FAPERJ,

JHEP03(2018)160

and FAPESP (Brazil); MES (Bulgaria); CERN; CAS, MoST, and NSFC (China); COLCIENCIAS (Colombia); MSES and CSF (Croatia); RPF (Cyprus); SENESCYT (Ecuador); MoER, ERC IUT, and ERDF (Estonia); Academy of Finland, MEC, and HIP (Finland); CEA and CNRS/IN2P3 (France); BMBF, DFG, and HGF (Germany); GSRT (Greece); OTKA and NIH (Hungary); DAE and DST (India); IPM (Iran); SFI (Ireland); INFN (Italy); MSIP and NRF (Republic of Korea); LAS (Lithuania); MOE and UM (Malaysia); BUAP, CINVESTAV, CONACYT, LNS, SEP, and UASLP-FAI (Mexico); MBIE (New Zealand); PAEC (Pakistan); MSHE and NSC (Poland); FCT (Portugal); JINR (Dubna); MON, RosAtom, RAS, RFBR and RAEP (Russia); MESTD (Serbia); SEIDI, CPAN, PCTI and FEDER (Spain); Swiss Funding Agencies (Switzerland); MST (Taipei); ThEPCenter, IPST, STAR, and NSTDA (Thailand); TUBITAK and TAEK (Turkey); NASU and SFFR (Ukraine); STFC (United Kingdom); DOE and NSF (USA).

Individuals have received support from the Marie-Curie program and the European Research Council and Horizon 2020 Grant, contract No. 675440 (European Union); the Leventis Foundation; the A. P. Sloan Foundation; the Alexander von Humboldt Foundation; the Belgian Federal Science Policy Office; the Fonds pour la Formation à la Recherche dans l'Industrie et dans l'Agriculture (FRIA-Belgium); the Agentschap voor Innovatie door Wetenschap en Technologie (IWT-Belgium); the Ministry of Education, Youth and Sports (MEYS) of the Czech Republic; the Council of Science and Industrial Research, India; the HOMING PLUS program of the Foundation for Polish Science, cofinanced from European Union, Regional Development Fund, the Mobility Plus program of the Ministry of Science and Higher Education, the National Science Center (Poland), contracts Harmonia 2014/14/M/ST2/00428, Opus 2014/13/B/ST2/02543, 2014/15/B/ST2/03998, and 2015/19/B/ST2/02861, Sonata-bis 2012/07/E/ST2/01406; the National Priorities Research Program by Qatar National Research Fund; the Programa Severo Ochoa del Principado de Asturias; the Thalis and Aristeia programs cofinanced by EU-ESF and the Greek NSRF; the Rachadapisek Sompot Fund for Postdoctoral Fellowship, Chulalongkorn University and the Chulalongkorn Academic into Its 2nd Century Project Advancement Project (Thailand); the Welch Foundation, contract C-1845; and the Weston Havens Foundation (USA).

References

[1] P. Ramond, *Dual theory for free fermions*, Phys. Rev. **D 3** (1971) 2415 [INSPIRE].

[2] Yu. A. Gol'fand and E.P. Likhtman, *Extension of the algebra of Poincaré group generators and violation of P invariance*, *JETP Lett.* **13** (1971) 323, http://www.jetpletters.ac.ru/ps/1584/article_24309.pdf [INSPIRE].

[3] A. Neveu and J.H. Schwarz, *Factorizable dual model of pions*, Nucl. Phys. **B 31** (1971) 86 [INSPIRE].

[4] D.V. Volkov and V.P. Akulov, *Possible universal neutrino interaction*, *JETP Lett.* **16** (1972) 438 [INSPIRE].

[5] J. Wess and B. Zumino, *A lagrangian model invariant under supergauge transformations*, *Phys. Lett.* **49B** (1974) 52 [INSPIRE].

[6] J. Wess and B. Zumino, *Supergauge transformations in four-dimensions*, *Nucl. Phys.* **B 70** (1974) 39 [INSPIRE].

[7] P. Fayet, *Supergauge invariant extension of the Higgs mechanism and a model for the electron and its neutrino*, *Nucl. Phys.* **B 90** (1975) 104 [INSPIRE].

[8] H.P. Nilles, *Supersymmetry, supergravity and particle physics*, *Phys. Rept.* **110** (1984) 1 [INSPIRE].

[9] S. Dimopoulos and G.F. Giudice, *Naturalness constraints in supersymmetric theories with nonuniversal soft terms*, *Phys. Lett.* **B 357** (1995) 573 [hep-ph/9507282] [INSPIRE].

[10] R. Barbieri and D. Pappadopulo, *S-particles at their naturalness limits*, *JHEP* **10** (2009) 061 [arXiv:0906.4546] [INSPIRE].

[11] M. Papucci, J.T. Ruderman and A. Weiler, *Natural SUSY endures*, *JHEP* **09** (2012) 035 [arXiv:1110.6926] [INSPIRE].

[12] A.J. Buras, J.R. Ellis, M.K. Gaillard and D.V. Nanopoulos, *Aspects of the grand unification of strong, weak and electromagnetic interactions*, *Nucl. Phys.* **B 135** (1978) 66 [INSPIRE].

[13] H.E. Haber and G.L. Kane, *The search for supersymmetry: probing physics beyond the standard model*, *Phys. Rept.* **117** (1985) 75 [INSPIRE].

[14] G.R. Farrar and P. Fayet, *Phenomenology of the production, decay and detection of new hadronic states associated with supersymmetry*, *Phys. Lett.* **76B** (1978) 575 [INSPIRE].

[15] H. Goldberg, *Constraint on the photino mass from cosmology*, *Phys. Rev. Lett.* **50** (1983) 1419 [*Erratum ibid.* **103** (2009) 099905] [INSPIRE].

[16] J.R. Ellis, J.S. Hagelin, D.V. Nanopoulos, K.A. Olive and M. Srednicki, *Supersymmetric relics from the big bang*, *Nucl. Phys.* **B 238** (1984) 453 [INSPIRE].

[17] Joint LEP2 SUSY Working Group, the ALEPH, DELPHI, L3 and OPAL collaborations, http://lepsusy.web.cern.ch/lepsusy/.

[18] ATLAS collaboration, *Search for electroweak production of supersymmetric states in scenarios with compressed mass spectra at* $\sqrt{s} = 13$ *TeV with the ATLAS detector*, *Submitted to: Phys. Rev. D* (2017) [arXiv:1712.08119] [INSPIRE].

[19] ATLAS collaboration, *Search for the electroweak production of supersymmetric particles in* $\sqrt{s} = 8$ *TeV pp collisions with the ATLAS detector*, *Phys. Rev.* **D 93** (2016) 052002 [arXiv:1509.07152] [INSPIRE].

[20] ATLAS collaboration, *Search for photonic signatures of gauge-mediated supersymmetry in 8 TeV pp collisions with the ATLAS detector*, *Phys. Rev.* **D 92** (2015) 072001 [arXiv:1507.05493] [INSPIRE].

[21] ATLAS collaboration, *Search for metastable heavy charged particles with large ionisation energy loss in pp collisions at* $\sqrt{s} = 8$ *TeV using the ATLAS experiment*, *Eur. Phys. J.* **C 75** (2015) 407 [arXiv:1506.05332] [INSPIRE].

[22] ATLAS collaboration, *Search for direct pair production of a chargino and a neutralino decaying to the 125 GeV Higgs boson in* $\sqrt{s} = 8$ *TeV pp collisions with the ATLAS detector*, *Eur. Phys. J.* **C 75** (2015) 208 [arXiv:1501.07110] [INSPIRE].

[23] ATLAS collaboration, *Searches for heavy long-lived charged particles with the ATLAS*

JHEP03(2018)160

detector in proton-proton collisions at $\sqrt{s} = 8$ *TeV*, *JHEP* **01** (2015) 068 [arXiv:1411.6795] [INSPIRE].

[24] ATLAS collaboration, *Search for nonpointing and delayed photons in the diphoton and missing transverse momentum final state in 8 TeV pp collisions at the LHC using the ATLAS detector*, *Phys. Rev.* **D 90** (2014) 112005 [arXiv:1409.5542] [INSPIRE].

[25] ATLAS collaboration, *Search for the direct production of charginos, neutralinos and staus in final states with at least two hadronically decaying taus and missing transverse momentum in pp collisions at* $\sqrt{s} = 8$ *TeV with the ATLAS detector*, *JHEP* **10** (2014) 096 [arXiv:1407.0350] [INSPIRE].

[26] ATLAS collaboration, *Search for supersymmetry in events with four or more leptons in* $\sqrt{s} = 8$ *TeV pp collisions with the ATLAS detector*, *Phys. Rev.* **D 90** (2014) 052001 [arXiv:1405.5086] [INSPIRE].

[27] ATLAS collaboration, *Search for direct production of charginos, neutralinos and sleptons in final states with two leptons and missing transverse momentum in pp collisions at* $\sqrt{s} = 8$ *TeV with the ATLAS detector*, *JHEP* **05** (2014) 071 [arXiv:1403.5294] [INSPIRE].

[28] ATLAS collaboration, *Search for direct production of charginos and neutralinos in events with three leptons and missing transverse momentum in* $\sqrt{s} = 8$ *TeV pp collisions with the ATLAS detector*, *JHEP* **04** (2014) 169 [arXiv:1402.7029] [INSPIRE].

[29] ATLAS collaboration, *Search for charginos nearly mass degenerate with the lightest neutralino based on a disappearing-track signature in pp collisions at* $\sqrt{s} = 8$ *TeV with the ATLAS detector*, *Phys. Rev.* **D 88** (2013) 112006 [arXiv:1310.3675] [INSPIRE].

[30] CMS collaboration, *Searches for electroweak production of charginos, neutralinos and sleptons decaying to leptons and W, Z and Higgs bosons in pp collisions at 8 TeV*, *Eur. Phys. J.* **C 74** (2014) 3036 [arXiv:1405.7570] [INSPIRE].

[31] CMS collaboration, *Searches for electroweak neutralino and chargino production in channels with Higgs, Z and W bosons in pp collisions at 8 TeV*, *Phys. Rev.* **D 90** (2014) 092007 [arXiv:1409.3168] [INSPIRE].

[32] CMS collaboration, *Search for supersymmetry in electroweak production with photons and large missing transverse energy in pp collisions at* $\sqrt{s} = 8$ *TeV*, *Phys. Lett.* **B 759** (2016) 479 [arXiv:1602.08772] [INSPIRE].

[33] CMS collaboration, *Search for supersymmetry in events with soft leptons, low jet multiplicity and missing transverse energy in proton–proton collisions at* $\sqrt{s} = 8$ *TeV*, *Phys. Lett.* **B 759** (2016) 9 [arXiv:1512.08002] [INSPIRE].

[34] CMS collaboration, *Search for supersymmetry in events with a photon, a lepton and missing transverse momentum in pp collisions at* $\sqrt{s} = 8$ *TeV*, *Phys. Lett.* **B 757** (2016) 6 [arXiv:1508.01218] [INSPIRE].

[35] CMS collaboration, *Search for electroweak production of charginos in final states with two* τ *leptons in pp collisions at* $\sqrt{s} = 8$ *TeV*, *JHEP* **04** (2017) 018 [arXiv:1610.04870] [INSPIRE].

[36] CMS collaboration, *Searches for long-lived charged particles in pp collisions at* $\sqrt{s} = 7$ *and* 8 *TeV*, *JHEP* **07** (2013) 122 [arXiv:1305.0491] [INSPIRE].

[37] CMS collaboration, *Search for disappearing tracks in proton-proton collisions at* $\sqrt{s} = 8$ *TeV*, *JHEP* **01** (2015) 096 [arXiv:1411.6006] [INSPIRE].

[38] CMS collaboration, *Search for electroweak production of charginos and neutralinos in multilepton final states in proton-proton collisions at* $\sqrt{s} = 13$ *TeV*, arXiv:1709.05406 [INSPIRE].

[39] CMS collaboration, *Search for new physics in events with two soft oppositely charged leptons and missing transverse momentum in proton-proton collisions at* $\sqrt{s} = 13$ *TeV*, arXiv:1801.01846 [INSPIRE].

[40] CMS collaboration, *Search for supersymmetry with Higgs boson to diphoton decays using the razor variables at* $\sqrt{s} = 13$ *TeV*, *Phys. Lett.* **B 779** (2018) 166 [arXiv:1709.00384] [INSPIRE].

[41] CMS collaboration, *Search for Higgsino pair production in pp collisions at* $\sqrt{s} = 13$ *TeV in final states with large missing transverse momentum and two Higgs bosons decaying via* $H \to b\bar{b}$, *Phys. Rev.* **D 97** (2018) 032007 [arXiv:1709.04896] [INSPIRE].

[42] CMS collaboration, *Search for new phenomena in final states with two opposite-charge, same-flavor leptons, jets and missing transverse momentum in pp collisions at* $\sqrt{s} = 13$ *TeV*, arXiv:1709.08908 [INSPIRE].

[43] CMS collaboration, *Search for electroweak production of charginos and neutralinos in WH events in proton-proton collisions at* $\sqrt{s} = 13$ *TeV*, *JHEP* **11** (2017) 029 [arXiv:1706.09933] [INSPIRE].

[44] J. Alwall, P. Schuster and N. Toro, *Simplified Models for a First Characterization of New Physics at the LHC*, *Phys. Rev.* **D 79** (2009) 075020 [arXiv:0810.3921] [INSPIRE].

[45] J. Alwall, M.-P. Le, M. Lisanti and J.G. Wacker, *Model-Independent Jets plus Missing Energy Searches*, *Phys. Rev.* **D 79** (2009) 015005 [arXiv:0809.3264] [INSPIRE].

[46] LHC New Physics Working Group collaboration, D. Alves, *Simplified Models for LHC New Physics Searches*, *J. Phys.* **G 39** (2012) 105005 [arXiv:1105.2838] [INSPIRE].

[47] CMS collaboration, *Interpretation of Searches for Supersymmetry with simplified Models*, *Phys. Rev.* **D 88** (2013) 052017 [arXiv:1301.2175] [INSPIRE].

[48] ATLAS, CMS collaboration, G. Aad et al., *Measurements of the Higgs boson production and decay rates and constraints on its couplings from a combined ATLAS and CMS analysis of the LHC pp collision data at* $\sqrt{s} = 7$ *and* 8 *TeV*, *JHEP* **08** (2016) 045 [arXiv:1606.02266] [INSPIRE].

[49] S.P. Martin, *A Supersymmetry primer*, hep-ph/9709356 [INSPIRE].

[50] K.T. Matchev and S.D. Thomas, *Higgs and Z boson signatures of supersymmetry*, *Phys. Rev.* **D 62** (2000) 077702 [hep-ph/9908482] [INSPIRE].

[51] P. Meade, M. Reece and D. Shih, *Prompt decays of general neutralino NLSPs at the Tevatron*, *JHEP* **05** (2010) 105 [arXiv:0911.4130] [INSPIRE].

[52] J.T. Ruderman and D. Shih, *General neutralino NLSPs at the early LHC*, *JHEP* **08** (2012) 159 [arXiv:1103.6083] [INSPIRE].

[53] P.Z. Skands et al., *SUSY Les Houches accord: Interfacing SUSY spectrum calculators, decay packages and event generators*, *JHEP* **07** (2004) 036 [hep-ph/0311123] [INSPIRE].

[54] W. Beenakker, M. Klasen, M. Krämer, T. Plehn, M. Spira and P.M. Zerwas, *Production of charginos/neutralinos and sleptons at hadron colliders*, *Phys. Rev. Lett.* **83** (1999) 3780 [*Erratum ibid.* **100** (2008) 029901] [hep-ph/9906298] [INSPIRE].

[55] B. Fuks, M. Klasen, D.R. Lamprea and M. Rothering, *Gaugino production in proton-proton collisions at a center-of-mass energy of 8 TeV*, *JHEP* **10** (2012) 081 [arXiv:1207.2159] [INSPIRE].

[56] B. Fuks, M. Klasen, D.R. Lamprea and M. Rothering, *Precision predictions for electroweak superpartner production at hadron colliders with Resummino*, *Eur. Phys. J.* **C 73** (2013)

2480 [arXiv:1304.0790] [INSPIRE].

[57] G. Bozzi, B. Fuks and M. Klasen, *Joint resummation for slepton pair production at hadron colliders*, *Nucl. Phys.* **B 794** (2008) 46 [arXiv:0709.3057] [INSPIRE].

[58] G. Bozzi, B. Fuks and M. Klasen, *Threshold resummation for slepton-pair production at hadron colliders*, *Nucl. Phys.* **B 777** (2007) 157 [hep-ph/0701202] [INSPIRE].

[59] G. Bozzi, B. Fuks and M. Klasen, *Transverse-momentum resummation for slepton-pair production at the CERN LHC*, *Phys. Rev.* **D 74** (2006) 015001 [hep-ph/0603074] [INSPIRE].

[60] CMS collaboration, *The CMS experiment at the CERN LHC*, 2008 *JINST* **3** S08004 [INSPIRE].

[61] CMS collaboration, *Particle-flow reconstruction and global event description with the CMS detector*, 2017 *JINST* **12** P10003 [arXiv:1706.04965] [INSPIRE].

[62] M. Cacciari, G.P. Salam and G. Soyez, *The anti-k_t jet clustering algorithm*, *JHEP* **04** (2008) 063 [arXiv:0802.1189] [INSPIRE].

[63] M. Cacciari, G.P. Salam and G. Soyez, *FastJet user manual*, *Eur. Phys. J.* **C 72** (2012) 1896 [arXiv:1111.6097] [INSPIRE].

[64] CMS collaboration, *Performance of the CMS missing transverse momentum reconstruction in pp data at $\sqrt{s} = 8$ TeV*, 2015 *JINST* **10** P02006 [arXiv:1411.0511] [INSPIRE].

[65] CMS collaboration, *Performance of Electron Reconstruction and Selection with the CMS Detector in Proton-Proton Collisions at $\sqrt{s} = 8$ TeV*, 2015 *JINST* **10** P06005 [arXiv:1502.02701] [INSPIRE].

[66] CMS collaboration, *Performance of CMS muon reconstruction in pp collision events at $\sqrt{s} = 7$ TeV*, 2012 *JINST* **7** P10002 [arXiv:1206.4071] [INSPIRE].

[67] CMS collaboration, *Reconstruction and identification of τ lepton decays to hadrons and ν_τ at CMS*, 2016 *JINST* **11** P01019 [arXiv:1510.07488] [INSPIRE].

[68] CMS collaboration, *Identification of heavy-flavour jets with the CMS detector in pp collisions at 13 TeV*, *Submitted to: JINST* (2017) [arXiv:1712.07158] [INSPIRE].

[69] D. Guest, J. Collado, P. Baldi, S.-C. Hsu, G. Urban and D. Whiteson, *Jet Flavor Classification in High-Energy Physics with Deep Neural Networks*, *Phys. Rev.* **D 94** (2016) 112002 [arXiv:1607.08633] [INSPIRE].

[70] J. Alwall et al., *The automated computation of tree-level and next-to-leading order differential cross sections and their matching to parton shower simulations*, *JHEP* **07** (2014) 079 [arXiv:1405.0301] [INSPIRE].

[71] T. Melia, P. Nason, R. Rontsch and G. Zanderighi, *W^+W^-, WZ and ZZ production in the POWHEG BOX*, *JHEP* **11** (2011) 078 [arXiv:1107.5051] [INSPIRE].

[72] P. Nason and G. Zanderighi, *W^+W^- , WZ and ZZ production in the POWHEG-BOX-V2*, *Eur. Phys. J.* **C 74** (2014) 2702 [arXiv:1311.1365] [INSPIRE].

[73] NNPDF collaboration, R.D. Ball et al., *Parton distributions for the LHC Run II*, *JHEP* **04** (2015) 040 [arXiv:1410.8849] [INSPIRE].

[74] T. Sjöstrand, S. Mrenna and P.Z. Skands, *A brief introduction to PYTHIA 8.1*, *Comput. Phys. Commun.* **178** (2008) 852 [arXiv:0710.3820] [INSPIRE].

[75] CMS collaboration, *Event generator tunes obtained from underlying event and multiparton scattering measurements*, *Eur. Phys. J.* **C 76** (2016) 155 [arXiv:1512.00815] [INSPIRE].

[76] J. Alwall et al., *Comparative study of various algorithms for the merging of parton showers and matrix elements in hadronic collisions*, *Eur. Phys. J.* **C 53** (2008) 473

[arXiv:0706.2569] [INSPIRE].

[77] R. Frederix and S. Frixione, *Merging meets matching in MC@NLO*, JHEP **12** (2012) 061 [arXiv:1209.6215] [INSPIRE].

[78] S. Alioli, P. Nason, C. Oleari and E. Re, *NLO single-top production matched with shower in POWHEG: s- and t-channel contributions*, JHEP **09** (2009) 111 [*Erratum ibid.* **1002** (2010) 011] [arXiv:0907.4076] [INSPIRE].

[79] E. Re, *Single-top Wt-channel production matched with parton showers using the POWHEG method*, Eur. Phys. J. **C 71** (2011) 1547 [arXiv:1009.2450] [INSPIRE].

[80] R. Gavin, Y. Li, F. Petriello and S. Quackenbush, *FEWZ 2.0: A code for hadronic Z production at next-to-next-to-leading order*, Comput. Phys. Commun. **182** (2011) 2388 [arXiv:1011.3540] [INSPIRE].

[81] R. Gavin, Y. Li, F. Petriello and S. Quackenbush, *W physics at the LHC with FEWZ 2.1*, Comput. Phys. Commun. **184** (2013) 208 [arXiv:1201.5896] [INSPIRE].

[82] M. Czakon and A. Mitov, *Top++: a program for the calculation of the top-pair cross-section at hadron colliders*, Comput. Phys. Commun. **185** (2014) 2930 [arXiv:1112.5675] [INSPIRE].

[83] C. Borschensky et al., *Squark and gluino production cross sections in pp collisions at* $\sqrt{s} = 13, 14, 33$ *and* 100 *TeV*, Eur. Phys. J. **C 74** (2014) 3174 [arXiv:1407.5066] [INSPIRE].

[84] CMS collaboration, *Search for top-squark pair production in the single-lepton final state in pp collisions at* $\sqrt{s} = 8$ *TeV*, Eur. Phys. J. **C 73** (2013) 2677 [arXiv:1308.1586] [INSPIRE].

[85] GEANT4 collaboration, S. Agostinelli et al., *GEANT4: a simulation toolkit*, Nucl. Instrum. Meth. **A 506** (2003) 250 [INSPIRE].

[86] S. Abdullin et al., *The fast simulation of the CMS detector at LHC*, J. Phys. Conf. Ser. **331** (2011) 032049 [INSPIRE].

[87] CMS collaboration, *Inclusive search for supersymmetry using the razor variables in pp collisions at* $\sqrt{s} = 7$ *TeV*, Phys. Rev. Lett. **111** (2013) 081802 [arXiv:1212.6961] [INSPIRE].

[88] CMS collaboration, *Search for supersymmetry with razor variables in pp collisions at* $\sqrt{s} = 7$ *TeV*, Phys. Rev. **D 90** (2014) 112001 [arXiv:1405.3961] [INSPIRE].

[89] CMS collaboration, *Search for new physics in same-sign dilepton events in proton-proton collisions at* $\sqrt{s} = 13$ *TeV*, Eur. Phys. J. **C 76** (2016) 439 [arXiv:1605.03171] [INSPIRE].

[90] T. Junk, *Confidence level computation for combining searches with small statistics*, Nucl. Instrum. Meth. **A 434** (1999) 435 [hep-ex/9902006] [INSPIRE].

[91] A.L. Read, *Presentation of search results: The* CL_s *technique*, J. Phys. **G 28** (2002) 2693 [INSPIRE].

[92] G. Cowan, K. Cranmer, E. Gross and O. Vitells, *Asymptotic formulae for likelihood-based tests of new physics*, Eur. Phys. J. **C 71** (2011) 1554 [*Erratum ibid.* **C 73** (2013) 2501] [arXiv:1007.1727] [INSPIRE].

[93] ATLAS and CMS collaborations, *Procedure for the LHC Higgs boson search combination in summer 2011*, ATL-PHYS-PUB-2011-011 (2011).

The CMS collaboration

Yerevan Physics Institute, Yerevan, Armenia

A.M. Sirunyan, A. Tumasyan

Institut für Hochenergiephysik, Wien, Austria

W. Adam, F. Ambrogi, E. Asilar, T. Bergauer, J. Brandstetter, E. Brondolin, M. Dragicevic, J. Erö, M. Flechl, M. Friedl, R. Frühwirth[1], V.M. Ghete, J. Grossmann, J. Hrubec, M. Jeitler[1], A. König, N. Krammer, I. Krätschmer, D. Liko, T. Madlener, I. Mikulec, E. Pree, N. Rad, H. Rohringer, J. Schieck[1], R. Schöfbeck, M. Spanring, D. Spitzbart, W. Waltenberger, J. Wittmann, C.-E. Wulz[1], M. Zarucki

Institute for Nuclear Problems, Minsk, Belarus

V. Chekhovsky, V. Mossolov, J. Suarez Gonzalez

Universiteit Antwerpen, Antwerpen, Belgium

E.A. De Wolf, D. Di Croce, X. Janssen, J. Lauwers, M. Van De Klundert, H. Van Haevermaet, P. Van Mechelen, N. Van Remortel

Vrije Universiteit Brussel, Brussel, Belgium

S. Abu Zeid, F. Blekman, J. D'Hondt, I. De Bruyn, J. De Clercq, K. Deroover, G. Flouris, D. Lontkovskyi, S. Lowette, I. Marchesini, S. Moortgat, L. Moreels, Q. Python, K. Skovpen, S. Tavernier, W. Van Doninck, P. Van Mulders, I. Van Parijs

Université Libre de Bruxelles, Bruxelles, Belgium

D. Beghin, H. Brun, B. Clerbaux, G. De Lentdecker, H. Delannoy, B. Dorney, G. Fasanella, L. Favart, R. Goldouzian, A. Grebenyuk, T. Lenzi, J. Luetic, T. Maerschalk, A. Marinov, T. Seva, E. Starling, C. Vander Velde, P. Vanlaer, D. Vannerom, R. Yonamine, F. Zenoni, F. Zhang[2]

Ghent University, Ghent, Belgium

A. Cimmino, T. Cornelis, D. Dobur, A. Fagot, M. Gul, I. Khvastunov[3], D. Poyraz, C. Roskas, S. Salva, M. Tytgat, W. Verbeke, N. Zaganidis

Université Catholique de Louvain, Louvain-la-Neuve, Belgium

H. Bakhshiansohi, O. Bondu, S. Brochet, G. Bruno, C. Caputo, A. Caudron, P. David, S. De Visscher, C. Delaere, M. Delcourt, B. Francois, A. Giammanco, M. Komm, G. Krintiras, V. Lemaitre, A. Magitteri, A. Mertens, M. Musich, K. Piotrzkowski, L. Quertenmont, A. Saggio, M. Vidal Marono, S. Wertz, J. Zobec

Centro Brasileiro de Pesquisas Fisicas, Rio de Janeiro, Brazil

W.L. Aldá Júnior, F.L. Alves, G.A. Alves, L. Brito, M. Correa Martins Junior, C. Hensel, A. Moraes, M.E. Pol, P. Rebello Teles

Universidade do Estado do Rio de Janeiro, Rio de Janeiro, Brazil

E. Belchior Batista Das Chagas, W. Carvalho, J. Chinellato[4], E. Coelho, E.M. Da Costa, G.G. Da Silveira[5], D. De Jesus Damiao, S. Fonseca De Souza, L.M. Huertas Guativa, H. Malbouisson, M. Melo De Almeida, C. Mora Herrera, L. Mundim, H. Nogima,

JHEP03(2018)160

L.J. Sanchez Rosas, A. Santoro, A. Sznajder, M. Thiel, E.J. Tonelli Manganote[4], F. Torres Da Silva De Araujo, A. Vilela Pereira

Universidade Estadual Paulista [a], Universidade Federal do ABC [b], São Paulo, Brazil

S. Ahuja[a], C.A. Bernardes[a], T.R. Fernandez Perez Tomei[a], E.M. Gregores[b], P.G. Mercadante[b], S.F. Novaes[a], Sandra S. Padula[a], D. Romero Abad[b], J.C. Ruiz Vargas[a]

Institute for Nuclear Research and Nuclear Energy, Bulgarian Academy of Sciences, Sofia, Bulgaria

A. Aleksandrov, R. Hadjiiska, P. Iaydjiev, M. Misheva, M. Rodozov, M. Shopova, G. Sultanov

University of Sofia, Sofia, Bulgaria

A. Dimitrov, L. Litov, B. Pavlov, P. Petkov

Beihang University, Beijing, China

W. Fang[6], X. Gao[6], L. Yuan

Institute of High Energy Physics, Beijing, China

M. Ahmad, J.G. Bian, G.M. Chen, H.S. Chen, M. Chen, Y. Chen, C.H. Jiang, D. Leggat, H. Liao, Z. Liu, F. Romeo, S.M. Shaheen, A. Spiezia, J. Tao, C. Wang, Z. Wang, E. Yazgan, H. Zhang, S. Zhang, J. Zhao

State Key Laboratory of Nuclear Physics and Technology, Peking University, Beijing, China

Y. Ban, G. Chen, Q. Li, S. Liu, Y. Mao, S.J. Qian, D. Wang, Z. Xu

Universidad de Los Andes, Bogota, Colombia

C. Avila, A. Cabrera, C.A. Carrillo Montoya, L.F. Chaparro Sierra, C. Florez, C.F. González Hernández, J.D. Ruiz Alvarez, M.A. Segura Delgado

University of Split, Faculty of Electrical Engineering, Mechanical Engineering and Naval Architecture, Split, Croatia

B. Courbon, N. Godinovic, D. Lelas, I. Puljak, P.M. Ribeiro Cipriano, T. Sculac

University of Split, Faculty of Science, Split, Croatia

Z. Antunovic, M. Kovac

Institute Rudjer Boskovic, Zagreb, Croatia

V. Brigljevic, D. Ferencek, K. Kadija, B. Mesic, A. Starodumov[7], T. Susa

University of Cyprus, Nicosia, Cyprus

M.W. Ather, A. Attikis, G. Mavromanolakis, J. Mousa, C. Nicolaou, F. Ptochos, P.A. Razis, H. Rykaczewski

Charles University, Prague, Czech Republic

M. Finger[8], M. Finger Jr.[8]

Universidad San Francisco de Quito, Quito, Ecuador

E. Carrera Jarrin

JHEP03(2018)160

Academy of Scientific Research and Technology of the Arab Republic of Egypt, Egyptian Network of High Energy Physics, Cairo, Egypt
A.A. Abdelalim[9,10], Y. Mohammed[11], E. Salama[12,13]

National Institute of Chemical Physics and Biophysics, Tallinn, Estonia
R.K. Dewanjee, M. Kadastik, L. Perrini, M. Raidal, A. Tiko, C. Veelken

Department of Physics, University of Helsinki, Helsinki, Finland
P. Eerola, H. Kirschenmann, J. Pekkanen, M. Voutilainen

Helsinki Institute of Physics, Helsinki, Finland
J. Havukainen, J.K. Heikkilä, T. Järvinen, V. Karimäki, R. Kinnunen, T. Lampén, K. Lassila-Perini, S. Laurila, S. Lehti, T. Lindén, P. Luukka, H. Siikonen, E. Tuominen, J. Tuominiemi

Lappeenranta University of Technology, Lappeenranta, Finland
T. Tuuva

IRFU, CEA, Université Paris-Saclay, Gif-sur-Yvette, France
M. Besancon, F. Couderc, M. Dejardin, D. Denegri, J.L. Faure, F. Ferri, S. Ganjour, S. Ghosh, P. Gras, G. Hamel de Monchenault, P. Jarry, I. Kucher, C. Leloup, E. Locci, M. Machet, J. Malcles, G. Negro, J. Rander, A. Rosowsky, M.Ö. Sahin, M. Titov

Laboratoire Leprince-Ringuet, Ecole polytechnique, CNRS/IN2P3, Université Paris-Saclay, Palaiseau, France
A. Abdulsalam, C. Amendola, I. Antropov, S. Baffioni, F. Beaudette, P. Busson, L. Cadamuro, C. Charlot, R. Granier de Cassagnac, M. Jo, S. Lisniak, A. Lobanov, J. Martin Blanco, M. Nguyen, C. Ochando, G. Ortona, P. Paganini, P. Pigard, R. Salerno, J.B. Sauvan, Y. Sirois, A.G. Stahl Leiton, T. Strebler, Y. Yilmaz, A. Zabi, A. Zghiche

Université de Strasbourg, CNRS, IPHC UMR 7178, F-67000 Strasbourg, France
J.-L. Agram[14], J. Andrea, D. Bloch, J.-M. Brom, M. Buttignol, E.C. Chabert, N. Chanon, C. Collard, E. Conte[14], X. Coubez, J.-C. Fontaine[14], D. Gelé, U. Goerlach, M. Jansová, A.-C. Le Bihan, N. Tonon, P. Van Hove

Centre de Calcul de l'Institut National de Physique Nucleaire et de Physique des Particules, CNRS/IN2P3, Villeurbanne, France
S. Gadrat

Université de Lyon, Université Claude Bernard Lyon 1, CNRS-IN2P3, Institut de Physique Nucléaire de Lyon, Villeurbanne, France
S. Beauceron, C. Bernet, G. Boudoul, R. Chierici, D. Contardo, P. Depasse, H. El Mamouni, J. Fay, L. Finco, S. Gascon, M. Gouzevitch, G. Grenier, B. Ille, F. Lagarde, I.B. Laktineh, M. Lethuillier, L. Mirabito, A.L. Pequegnot, S. Perries, A. Popov[15], V. Sordini, M. Vander Donckt, S. Viret

Georgian Technical University, Tbilisi, Georgia
A. Khvedelidze[8]

JHEP03(2018)160

Tbilisi State University, Tbilisi, Georgia

Z. Tsamalaidze[8]

RWTH Aachen University, I. Physikalisches Institut, Aachen, Germany

C. Autermann, L. Feld, M.K. Kiesel, K. Klein, M. Lipinski, M. Preuten, C. Schomakers, J. Schulz, V. Zhukov[15]

RWTH Aachen University, III. Physikalisches Institut A, Aachen, Germany

A. Albert, E. Dietz-Laursonn, D. Duchardt, M. Endres, M. Erdmann, S. Erdweg, T. Esch, R. Fischer, A. Güth, M. Hamer, T. Hebbeker, C. Heidemann, K. Hoepfner, S. Knutzen, M. Merschmeyer, A. Meyer, P. Millet, S. Mukherjee, T. Pook, M. Radziej, H. Reithler, M. Rieger, F. Scheuch, D. Teyssier, S. Thüer

RWTH Aachen University, III. Physikalisches Institut B, Aachen, Germany

G. Flügge, B. Kargoll, T. Kress, A. Künsken, T. Müller, A. Nehrkorn, A. Nowack, C. Pistone, O. Pooth, A. Stahl[16]

Deutsches Elektronen-Synchrotron, Hamburg, Germany

M. Aldaya Martin, T. Arndt, C. Asawatangtrakuldee, K. Beernaert, O. Behnke, U. Behrens, A. Bermúdez Martínez, A.A. Bin Anuar, K. Borras[17], V. Botta, A. Campbell, P. Connor, C. Contreras-Campana, F. Costanza, C. Diez Pardos, G. Eckerlin, D. Eckstein, T. Eichhorn, E. Eren, E. Gallo[18], J. Garay Garcia, A. Geiser, J.M. Grados Luyando, A. Grohsjean, P. Gunnellini, M. Guthoff, A. Harb, J. Hauk, M. Hempel[19], H. Jung, M. Kasemann, J. Keaveney, C. Kleinwort, I. Korol, D. Krücker, W. Lange, A. Lelek, T. Lenz, J. Leonard, K. Lipka, W. Lohmann[19], R. Mankel, I.-A. Melzer-Pellmann, A.B. Meyer, G. Mittag, J. Mnich, A. Mussgiller, E. Ntomari, D. Pitzl, A. Raspereza, M. Savitskyi, P. Saxena, R. Shevchenko, S. Spannagel, N. Stefaniuk, G.P. Van Onsem, R. Walsh, Y. Wen, K. Wichmann, C. Wissing, O. Zenaiev

University of Hamburg, Hamburg, Germany

R. Aggleton, S. Bein, V. Blobel, M. Centis Vignali, T. Dreyer, E. Garutti, D. Gonzalez, J. Haller, A. Hinzmann, M. Hoffmann, A. Karavdina, R. Klanner, R. Kogler, N. Kovalchuk, S. Kurz, T. Lapsien, D. Marconi, M. Meyer, M. Niedziela, D. Nowatschin, F. Pantaleo[16], T. Peiffer, A. Perieanu, C. Scharf, P. Schleper, A. Schmidt, S. Schumann, J. Schwandt, J. Sonneveld, H. Stadie, G. Steinbrück, F.M. Stober, M. Stöver, H. Tholen, D. Troendle, E. Usai, A. Vanhoefer, B. Vormwald

Institut für Experimentelle Kernphysik, Karlsruhe, Germany

M. Akbiyik, C. Barth, M. Baselga, S. Baur, E. Butz, R. Caspart, T. Chwalek, F. Colombo, W. De Boer, A. Dierlamm, N. Faltermann, B. Freund, R. Friese, M. Giffels, M.A. Harrendorf, F. Hartmann[16], S.M. Heindl, U. Husemann, F. Kassel[16], S. Kudella, H. Mildner, M.U. Mozer, Th. Müller, M. Plagge, G. Quast, K. Rabbertz, M. Schröder, I. Shvetsov, G. Sieber, H.J. Simonis, R. Ulrich, S. Wayand, M. Weber, T. Weiler, S. Williamson, C. Wöhrmann, R. Wolf

JHEP03(2018)160

Institute of Nuclear and Particle Physics (INPP), NCSR Demokritos, Aghia Paraskevi, Greece
G. Anagnostou, G. Daskalakis, T. Geralis, A. Kyriakis, D. Loukas, I. Topsis-Giotis

National and Kapodistrian University of Athens, Athens, Greece
G. Karathanasis, S. Kesisoglou, A. Panagiotou, N. Saoulidou

National Technical University of Athens, Athens, Greece
K. Kousouris

University of Ioánnina, Ioánnina, Greece
I. Evangelou, C. Foudas, P. Kokkas, S. Mallios, N. Manthos, I. Papadopoulos, E. Paradas, J. Strologas, F.A. Triantis

MTA-ELTE Lendület CMS Particle and Nuclear Physics Group, Eötvös Loránd University, Budapest, Hungary
M. Csanad, N. Filipovic, G. Pasztor, O. Surányi, G.I. Veres[20]

Wigner Research Centre for Physics, Budapest, Hungary
G. Bencze, C. Hajdu, D. Horvath[21], Á. Hunyadi, F. Sikler, V. Veszpremi

Institute of Nuclear Research ATOMKI, Debrecen, Hungary
N. Beni, S. Czellar, J. Karancsi[22], A. Makovec, J. Molnar, Z. Szillasi

Institute of Physics, University of Debrecen, Debrecen, Hungary
M. Bartók[20], P. Raics, Z.L. Trocsanyi, B. Ujvari

Indian Institute of Science (IISc), Bangalore, India
S. Choudhury, J.R. Komaragiri

National Institute of Science Education and Research, Bhubaneswar, India
S. Bahinipati[23], S. Bhowmik, P. Mal, K. Mandal, A. Nayak[24], D.K. Sahoo[23], N. Sahoo, S.K. Swain

Panjab University, Chandigarh, India
S. Bansal, S.B. Beri, V. Bhatnagar, R. Chawla, N. Dhingra, A.K. Kalsi, A. Kaur, M. Kaur, S. Kaur, R. Kumar, P. Kumari, A. Mehta, J.B. Singh, G. Walia

University of Delhi, Delhi, India
Ashok Kumar, Aashaq Shah, A. Bhardwaj, S. Chauhan, B.C. Choudhary, R.B. Garg, S. Keshri, A. Kumar, S. Malhotra, M. Naimuddin, K. Ranjan, R. Sharma

Saha Institute of Nuclear Physics, HBNI, Kolkata, India
R. Bhardwaj, R. Bhattacharya, S. Bhattacharya, U. Bhawandeep, S. Dey, S. Dutt, S. Dutta, S. Ghosh, N. Majumdar, A. Modak, K. Mondal, S. Mukhopadhyay, S. Nandan, A. Purohit, A. Roy, S. Roy Chowdhury, S. Sarkar, M. Sharan, S. Thakur

Indian Institute of Technology Madras, Madras, India
P.K. Behera

JHEP03(2018)160

Bhabha Atomic Research Centre, Mumbai, India

R. Chudasama, D. Dutta, V. Jha, V. Kumar, A.K. Mohanty[16], P.K. Netrakanti, L.M. Pant, P. Shukla, A. Topkar

Tata Institute of Fundamental Research-A, Mumbai, India

T. Aziz, S. Dugad, B. Mahakud, S. Mitra, G.B. Mohanty, N. Sur, B. Sutar

Tata Institute of Fundamental Research-B, Mumbai, India

S. Banerjee, S. Bhattacharya, S. Chatterjee, P. Das, M. Guchait, Sa. Jain, S. Kumar, M. Maity[25], G. Majumder, K. Mazumdar, T. Sarkar[25], N. Wickramage[26]

Indian Institute of Science Education and Research (IISER), Pune, India

S. Chauhan, S. Dube, V. Hegde, A. Kapoor, K. Kothekar, S. Pandey, A. Rane, S. Sharma

Institute for Research in Fundamental Sciences (IPM), Tehran, Iran

S. Chenarani[27], E. Eskandari Tadavani, S.M. Etesami[27], M. Khakzad, M. Mohammadi Najafabadi, M. Naseri, S. Paktinat Mehdiabadi[28], F. Rezaei Hosseinabadi, B. Safarzadeh[29], M. Zeinali

University College Dublin, Dublin, Ireland

M. Felcini, M. Grunewald

INFN Sezione di Bari [a], Università di Bari [b], Politecnico di Bari [c], Bari, Italy

M. Abbrescia[a,b], C. Calabria[a,b], A. Colaleo[a], D. Creanza[a,c], L. Cristella[a,b], N. De Filippis[a,c], M. De Palma[a,b], F. Errico[a,b], L. Fiore[a], G. Iaselli[a,c], S. Lezki[a,b], G. Maggi[a,c], M. Maggi[a], G. Miniello[a,b], S. My[a,b], S. Nuzzo[a,b], A. Pompili[a,b], G. Pugliese[a,c], R. Radogna[a], A. Ranieri[a], G. Selvaggi[a,b], A. Sharma[a], L. Silvestris[a,16], R. Venditti[a], P. Verwilligen[a]

INFN Sezione di Bologna [a], Università di Bologna [b], Bologna, Italy

G. Abbiendi[a], C. Battilana[a,b], D. Bonacorsi[a,b], L. Borgonovi[a,b], S. Braibant-Giacomelli[a,b], R. Campanini[a,b], P. Capiluppi[a,b], A. Castro[a,b], F.R. Cavallo[a], S.S. Chhibra[a], G. Codispoti[a,b], M. Cuffiani[a,b], G.M. Dallavalle[a], F. Fabbri[a], A. Fanfani[a,b], D. Fasanella[a,b], P. Giacomelli[a], C. Grandi[a], L. Guiducci[a,b], S. Marcellini[a], G. Masetti[a], A. Montanari[a], F.L. Navarria[a,b], A. Perrotta[a], A.M. Rossi[a,b], T. Rovelli[a,b], G.P. Siroli[a,b], N. Tosi[a]

INFN Sezione di Catania [a], Università di Catania [b], Catania, Italy

S. Albergo[a,b], S. Costa[a,b], A. Di Mattia[a], F. Giordano[a,b], R. Potenza[a,b], A. Tricomi[a,b], C. Tuve[a,b]

INFN Sezione di Firenze [a], Università di Firenze [b], Firenze, Italy

G. Barbagli[a], K. Chatterjee[a,b], V. Ciulli[a,b], C. Civinini[a], R. D'Alessandro[a,b], E. Focardi[a,b], P. Lenzi[a,b], M. Meschini[a], S. Paoletti[a], L. Russo[a,30], G. Sguazzoni[a], D. Strom[a], L. Viliani[a,b,16]

INFN Laboratori Nazionali di Frascati, Frascati, Italy

L. Benussi, S. Bianco, F. Fabbri, D. Piccolo, F. Primavera[16]

JHEP03(2018)160

INFN Sezione di Genova [a], Università di Genova [b], Genova, Italy
V. Calvelli[a,b], F. Ferro[a], E. Robutti[a], S. Tosi[a,b]

INFN Sezione di Milano-Bicocca [a], Università di Milano-Bicocca [b], Milano, Italy
A. Benaglia[a], A. Beschi[b], L. Brianza[a,b], F. Brivio[a,b], V. Ciriolo[a,b,16], M.E. Dinardo[a,b], S. Fiorendi[a,b], S. Gennai[a], A. Ghezzi[a,b], P. Govoni[a,b], M. Malberti[a,b], S. Malvezzi[a], R.A. Manzoni[a,b], D. Menasce[a], L. Moroni[a], M. Paganoni[a,b], K. Pauwels[a,b], D. Pedrini[a], S. Pigazzini[a,b,31], S. Ragazzi[a,b], T. Tabarelli de Fatis[a,b]

INFN Sezione di Napoli [a], Università di Napoli 'Federico II' [b], Napoli, Italy, Università della Basilicata [c], Potenza, Italy, Università G. Marconi [d], Roma, Italy
S. Buontempo[a], N. Cavallo[a,c], S. Di Guida[a,d,16], F. Fabozzi[a,c], F. Fienga[a,b], A.O.M. Iorio[a,b], W.A. Khan[a], L. Lista[a], S. Meola[a,d,16], P. Paolucci[a,16], C. Sciacca[a,b], F. Thyssen[a]

INFN Sezione di Padova [a], Università di Padova [b], Padova, Italy, Università di Trento [c], Trento, Italy
P. Azzi[a], N. Bacchetta[a], L. Benato[a,b], D. Bisello[a,b], A. Boletti[a,b], R. Carlin[a,b], A. Carvalho Antunes De Oliveira[a,b], P. Checchia[a], P. De Castro Manzano[a], T. Dorigo[a], U. Dosselli[a], F. Gasparini[a,b], U. Gasparini[a,b], A. Gozzelino[a], S. Lacaprara[a], M. Margoni[a,b], A.T. Meneguzzo[a,b], N. Pozzobon[a,b], P. Ronchese[a,b], R. Rossin[a,b], F. Simonetto[a,b], E. Torassa[a], M. Zanetti[a,b], P. Zotto[a,b], G. Zumerle[a,b]

INFN Sezione di Pavia [a], Università di Pavia [b], Pavia, Italy
A. Braghieri[a], A. Magnani[a], P. Montagna[a,b], S.P. Ratti[a,b], V. Re[a], M. Ressegotti[a,b], C. Riccardi[a,b], P. Salvini[a], I. Vai[a,b], P. Vitulo[a,b]

INFN Sezione di Perugia [a], Università di Perugia [b], Perugia, Italy
L. Alunni Solestizi[a,b], M. Biasini[a,b], G.M. Bilei[a], C. Cecchi[a,b], D. Ciangottini[a,b], L. Fanò[a,b], P. Lariccia[a,b], R. Leonardi[a,b], E. Manoni[a], G. Mantovani[a,b], V. Mariani[a,b], M. Menichelli[a], A. Rossi[a,b], A. Santocchia[a,b], D. Spiga[a]

INFN Sezione di Pisa [a], Università di Pisa [b], Scuola Normale Superiore di Pisa [c], Pisa, Italy
K. Androsov[a], P. Azzurri[a,16], G. Bagliesi[a], T. Boccali[a], L. Borrello, R. Castaldi[a], M.A. Ciocci[a,b], R. Dell'Orso[a], G. Fedi[a], L. Giannini[a,c], A. Giassi[a], M.T. Grippo[a,30], F. Ligabue[a,c], T. Lomtadze[a], E. Manca[a,c], G. Mandorli[a,c], A. Messineo[a,b], F. Palla[a], A. Rizzi[a,b], A. Savoy-Navarro[a,32], P. Spagnolo[a], R. Tenchini[a], G. Tonelli[a,b], A. Venturi[a], P.G. Verdini[a]

INFN Sezione di Roma [a], Sapienza Università di Roma [b], Rome, Italy
L. Barone[a,b], F. Cavallari[a], M. Cipriani[a,b], N. Daci[a], D. Del Re[a,b], E. Di Marco[a,b], M. Diemoz[a], S. Gelli[a,b], E. Longo[a,b], F. Margaroli[a,b], B. Marzocchi[a,b], P. Meridiani[a], G. Organtini[a,b], R. Paramatti[a,b], F. Preiato[a,b], S. Rahatlou[a,b], C. Rovelli[a], F. Santanastasio[a,b]

JHEP03(2018)160

INFN Sezione di Torino [a], Università di Torino [b], Torino, Italy, Università del Piemonte Orientale [c], Novara, Italy

N. Amapane[a,b], R. Arcidiacono[a,c], S. Argiro[a,b], M. Arneodo[a,c], N. Bartosik[a], R. Bellan[a,b], C. Biino[a], N. Cartiglia[a], F. Cenna[a,b], M. Costa[a,b], R. Covarelli[a,b], A. Degano[a,b], N. Demaria[a], B. Kiani[a,b], C. Mariotti[a], S. Maselli[a], E. Migliore[a,b], V. Monaco[a,b], E. Monteil[a,b], M. Monteno[a], M.M. Obertino[a,b], L. Pacher[a,b], N. Pastrone[a], M. Pelliccioni[a], G.L. Pinna Angioni[a,b], F. Ravera[a,b], A. Romero[a,b], M. Ruspa[a,c], R. Sacchi[a,b], K. Shchelina[a,b], V. Sola[a], A. Solano[a,b], A. Staiano[a], P. Traczyk[a,b]

INFN Sezione di Trieste [a], Università di Trieste [b], Trieste, Italy

S. Belforte[a], M. Casarsa[a], F. Cossutti[a], G. Della Ricca[a,b], A. Zanetti[a]

Kyungpook National University, Daegu, Korea

D.H. Kim, G.N. Kim, M.S. Kim, J. Lee, S. Lee, S.W. Lee, C.S. Moon, Y.D. Oh, S. Sekmen, D.C. Son, Y.C. Yang

Chonbuk National University, Jeonju, Korea

A. Lee

Chonnam National University, Institute for Universe and Elementary Particles, Kwangju, Korea

H. Kim, D.H. Moon, G. Oh

Hanyang University, Seoul, Korea

J.A. Brochero Cifuentes, J. Goh, T.J. Kim

Korea University, Seoul, Korea

S. Cho, S. Choi, Y. Go, D. Gyun, S. Ha, B. Hong, Y. Jo, Y. Kim, K. Lee, K.S. Lee, S. Lee, J. Lim, S.K. Park, Y. Roh

Seoul National University, Seoul, Korea

J. Almond, J. Kim, J.S. Kim, H. Lee, K. Lee, K. Nam, S.B. Oh, B.C. Radburn-Smith, S.h. Seo, U.K. Yang, H.D. Yoo, G.B. Yu

University of Seoul, Seoul, Korea

H. Kim, J.H. Kim, J.S.H. Lee, I.C. Park

Sungkyunkwan University, Suwon, Korea

Y. Choi, C. Hwang, J. Lee, I. Yu

Vilnius University, Vilnius, Lithuania

V. Dudenas, A. Juodagalvis, J. Vaitkus

National Centre for Particle Physics, Universiti Malaya, Kuala Lumpur, Malaysia

I. Ahmed, Z.A. Ibrahim, M.A.B. Md Ali[33], F. Mohamad Idris[34], W.A.T. Wan Abdullah, M.N. Yusli, Z. Zolkapli

JHEP03(2018)160

Centro de Investigacion y de Estudios Avanzados del IPN, Mexico City, Mexico
Reyes-Almanza, R, Ramirez-Sanchez, G., Duran-Osuna, M. C., H. Castilla-Valdez, E. De La Cruz-Burelo, I. Heredia-De La Cruz[35], Rabadan-Trejo, R. I., R. Lopez-Fernandez, J. Mejia Guisao, A. Sanchez-Hernandez

Universidad Iberoamericana, Mexico City, Mexico
S. Carrillo Moreno, C. Oropeza Barrera, F. Vazquez Valencia

Benemerita Universidad Autonoma de Puebla, Puebla, Mexico
J. Eysermans, I. Pedraza, H.A. Salazar Ibarguen, C. Uribe Estrada

Universidad Autónoma de San Luis Potosí, San Luis Potosí, Mexico
A. Morelos Pineda

University of Auckland, Auckland, New Zealand
D. Krofcheck

University of Canterbury, Christchurch, New Zealand
P.H. Butler

National Centre for Physics, Quaid-I-Azam University, Islamabad, Pakistan
A. Ahmad, M. Ahmad, Q. Hassan, H.R. Hoorani, A. Saddique, M.A. Shah, M. Shoaib, M. Waqas

National Centre for Nuclear Research, Swierk, Poland
H. Bialkowska, M. Bluj, B. Boimska, T. Frueboes, M. Górski, M. Kazana, K. Nawrocki, M. Szleper, P. Zalewski

Institute of Experimental Physics, Faculty of Physics, University of Warsaw, Warsaw, Poland
K. Bunkowski, A. Byszuk[36], K. Doroba, A. Kalinowski, M. Konecki, J. Krolikowski, M. Misiura, M. Olszewski, A. Pyskir, M. Walczak

Laboratório de Instrumentação e Física Experimental de Partículas, Lisboa, Portugal
P. Bargassa, C. Beirão Da Cruz E Silva, A. Di Francesco, P. Faccioli, B. Galinhas, M. Gallinaro, J. Hollar, N. Leonardo, L. Lloret Iglesias, M.V. Nemallapudi, J. Seixas, G. Strong, O. Toldaiev, D. Vadruccio, J. Varela

Joint Institute for Nuclear Research, Dubna, Russia
S. Afanasiev, V. Alexakhin, P. Bunin, M. Gavrilenko, A. Golunov, I. Golutvin, N. Gorbounov, V. Karjavin, A. Lanev, A. Malakhov, V. Matveev[37,38], V. Palichik, V. Perelygin, M. Savina, S. Shmatov, N. Skatchkov, V. Smirnov, A. Zarubin

Petersburg Nuclear Physics Institute, Gatchina (St. Petersburg), Russia
Y. Ivanov, V. Kim[39], E. Kuznetsova[40], P. Levchenko, V. Murzin, V. Oreshkin, I. Smirnov, V. Sulimov, L. Uvarov, S. Vavilov, A. Vorobyev

JHEP03(2018)160

Institute for Nuclear Research, Moscow, Russia
Yu. Andreev, A. Dermenev, S. Gninenko, N. Golubev, A. Karneyeu, M. Kirsanov, N. Krasnikov, A. Pashenkov, D. Tlisov, A. Toropin

Institute for Theoretical and Experimental Physics, Moscow, Russia
V. Epshteyn, V. Gavrilov, N. Lychkovskaya, V. Popov, I. Pozdnyakov, G. Safronov, A. Spiridonov, A. Stepennov, M. Toms, E. Vlasov, A. Zhokin

Moscow Institute of Physics and Technology, Moscow, Russia
T. Aushev, A. Bylinkin[38]

National Research Nuclear University 'Moscow Engineering Physics Institute' (MEPhI), Moscow, Russia
R. Chistov[41], M. Danilov[41], P. Parygin, D. Philippov, S. Polikarpov, E. Tarkovskii

P.N. Lebedev Physical Institute, Moscow, Russia
V. Andreev, M. Azarkin[38], I. Dremin[38], M. Kirakosyan[38], A. Terkulov

Skobeltsyn Institute of Nuclear Physics, Lomonosov Moscow State University, Moscow, Russia
A. Baskakov, A. Belyaev, E. Boos, M. Dubinin[42], L. Dudko, A. Ershov, A. Gribushin, V. Klyukhin, O. Kodolova, I. Lokhtin, I. Miagkov, S. Obraztsov, S. Petrushanko, V. Savrin, A. Snigirev

Novosibirsk State University (NSU), Novosibirsk, Russia
V. Blinov[43], D. Shtol[43], Y. Skovpen[43]

State Research Center of Russian Federation, Institute for High Energy Physics of NRC "Kurchatov Institute", Protvino, Russia
I. Azhgirey, I. Bayshev, S. Bitioukov, D. Elumakhov, V. Kachanov, A. Kalinin, D. Konstantinov, P. Mandrik, V. Petrov, R. Ryutin, A. Sobol, S. Troshin, N. Tyurin, A. Uzunian, A. Volkov

University of Belgrade, Faculty of Physics and Vinca Institute of Nuclear Sciences, Belgrade, Serbia
P. Adzic[44], P. Cirkovic, D. Devetak, M. Dordevic, J. Milosevic, V. Rekovic

Centro de Investigaciones Energéticas Medioambientales y Tecnológicas (CIEMAT), Madrid, Spain
J. Alcaraz Maestre, M. Barrio Luna, M. Cerrada, N. Colino, B. De La Cruz, A. Delgado Peris, A. Escalante Del Valle, C. Fernandez Bedoya, J.P. Fernández Ramos, J. Flix, M.C. Fouz, O. Gonzalez Lopez, S. Goy Lopez, J.M. Hernandez, M.I. Josa, D. Moran, A. Pérez-Calero Yzquierdo, J. Puerta Pelayo, A. Quintario Olmeda, I. Redondo, L. Romero, M.S. Soares, A. Álvarez Fernández

Universidad Autónoma de Madrid, Madrid, Spain
C. Albajar, J.F. de Trocóniz, M. Missiroli

Universidad de Oviedo, Oviedo, Spain

J. Cuevas, C. Erice, J. Fernandez Menendez, I. Gonzalez Caballero, J.R. González Fernández, E. Palencia Cortezon, S. Sanchez Cruz, P. Vischia, J.M. Vizan Garcia

Instituto de Física de Cantabria (IFCA), CSIC-Universidad de Cantabria, Santander, Spain

I.J. Cabrillo, A. Calderon, B. Chazin Quero, E. Curras, J. Duarte Campderros, M. Fernandez, J. Garcia-Ferrero, G. Gomez, A. Lopez Virto, J. Marco, C. Martinez Rivero, P. Martinez Ruiz del Arbol, F. Matorras, J. Piedra Gomez, T. Rodrigo, A. Ruiz-Jimeno, L. Scodellaro, N. Trevisani, I. Vila, R. Vilar Cortabitarte

CERN, European Organization for Nuclear Research, Geneva, Switzerland

D. Abbaneo, B. Akgun, E. Auffray, P. Baillon, A.H. Ball, D. Barney, J. Bendavid, M. Bianco, P. Bloch, A. Bocci, C. Botta, T. Camporesi, R. Castello, M. Cepeda, G. Cerminara, E. Chapon, Y. Chen, D. d'Enterria, A. Dabrowski, V. Daponte, A. David, M. De Gruttola, A. De Roeck, N. Deelen, M. Dobson, T. du Pree, M. Dünser, N. Dupont, A. Elliott-Peisert, P. Everaerts, F. Fallavollita, G. Franzoni, J. Fulcher, W. Funk, D. Gigi, A. Gilbert, K. Gill, F. Glege, D. Gulhan, P. Harris, J. Hegeman, V. Innocente, A. Jafari, P. Janot, O. Karacheban[19], J. Kieseler, V. Knünz, A. Kornmayer, M.J. Kortelainen, M. Krammer[1], C. Lange, P. Lecoq, C. Lourenço, M.T. Lucchini, L. Malgeri, M. Mannelli, A. Martelli, F. Meijers, J.A. Merlin, S. Mersi, E. Meschi, P. Milenovic[45], F. Moortgat, M. Mulders, H. Neugebauer, J. Ngadiuba, S. Orfanelli, L. Orsini, L. Pape, E. Perez, M. Peruzzi, A. Petrilli, G. Petrucciani, A. Pfeiffer, M. Pierini, D. Rabady, A. Racz, T. Reis, G. Rolandi[46], M. Rovere, H. Sakulin, C. Schäfer, C. Schwick, M. Seidel, M. Selvaggi, A. Sharma, P. Silva, P. Sphicas[47], A. Stakia, J. Steggemann, M. Stoye, M. Tosi, D. Treille, A. Triossi, A. Tsirou, V. Veckalns[48], M. Verweij, W.D. Zeuner

Paul Scherrer Institut, Villigen, Switzerland

W. Bertl[†], L. Caminada[49], K. Deiters, W. Erdmann, R. Horisberger, Q. Ingram, H.C. Kaestli, D. Kotlinski, U. Langenegger, T. Rohe, S.A. Wiederkehr

ETH Zurich - Institute for Particle Physics and Astrophysics (IPA), Zurich, Switzerland

M. Backhaus, L. Bäni, P. Berger, L. Bianchini, B. Casal, G. Dissertori, M. Dittmar, M. Donegà, C. Dorfer, C. Grab, C. Heidegger, D. Hits, J. Hoss, G. Kasieczka, T. Klijnsma, W. Lustermann, B. Mangano, M. Marionneau, M.T. Meinhard, D. Meister, F. Micheli, P. Musella, F. Nessi-Tedaldi, F. Pandolfi, J. Pata, F. Pauss, G. Perrin, L. Perrozzi, M. Quittnat, M. Reichmann, D.A. Sanz Becerra, M. Schönenberger, L. Shchutska, V.R. Tavolaro, K. Theofilatos, M.L. Vesterbacka Olsson, R. Wallny, D.H. Zhu

Universität Zürich, Zurich, Switzerland

T.K. Aarrestad, C. Amsler[50], M.F. Canelli, A. De Cosa, R. Del Burgo, S. Donato, C. Galloni, T. Hreus, B. Kilminster, D. Pinna, G. Rauco, P. Robmann, D. Salerno, K. Schweiger, C. Seitz, Y. Takahashi, A. Zucchetta

JHEP03(2018)160

National Central University, Chung-Li, Taiwan
V. Candelise, T.H. Doan, Sh. Jain, R. Khurana, C.M. Kuo, W. Lin, A. Pozdnyakov, S.S. Yu

National Taiwan University (NTU), Taipei, Taiwan
Arun Kumar, P. Chang, Y. Chao, K.F. Chen, P.H. Chen, F. Fiori, W.-S. Hou, Y. Hsiung, Y.F. Liu, R.-S. Lu, E. Paganis, A. Psallidas, A. Steen, J.f. Tsai

Chulalongkorn University, Faculty of Science, Department of Physics, Bangkok, Thailand
B. Asavapibhop, K. Kovitanggoon, G. Singh, N. Srimanobhas

Çukurova University, Physics Department, Science and Art Faculty, Adana, Turkey
M.N. Bakirci[51], A. Bat, F. Boran, S. Damarseckin, Z.S. Demiroglu, C. Dozen, E. Eskut, S. Girgis, G. Gokbulut, Y. Guler, I. Hos[52], E.E. Kangal[53], O. Kara, U. Kiminsu, M. Oglakci, G. Onengut[54], K. Ozdemir[55], S. Ozturk[51], A. Polatoz, D. Sunar Cerci[56], U.G. Tok, S. Turkcapar, I.S. Zorbakir, C. Zorbilmez

Middle East Technical University, Physics Department, Ankara, Turkey
B. Bilin, G. Karapinar[57], K. Ocalan[58], M. Yalvac, M. Zeyrek

Bogazici University, Istanbul, Turkey
E. Gülmez, M. Kaya[59], O. Kaya[60], S. Tekten, E.A. Yetkin[61]

Istanbul Technical University, Istanbul, Turkey
M.N. Agaras, S. Atay, A. Cakir, K. Cankocak, I. Köseoglu

Institute for Scintillation Materials of National Academy of Science of Ukraine, Kharkov, Ukraine
B. Grynyov

National Scientific Center, Kharkov Institute of Physics and Technology, Kharkov, Ukraine
L. Levchuk

University of Bristol, Bristol, U.K.
F. Ball, L. Beck, J.J. Brooke, D. Burns, E. Clement, D. Cussans, O. Davignon, H. Flacher, J. Goldstein, G.P. Heath, H.F. Heath, L. Kreczko, D.M. Newbold[62], S. Paramesvaran, T. Sakuma, S. Seif El Nasr-storey, D. Smith, V.J. Smith

Rutherford Appleton Laboratory, Didcot, U.K.
K.W. Bell, A. Belyaev[63], C. Brew, R.M. Brown, L. Calligaris, D. Cieri, D.J.A. Cockerill, J.A. Coughlan, K. Harder, S. Harper, J. Linacre, E. Olaiya, D. Petyt, C.H. Shepherd-Themistocleous, A. Thea, I.R. Tomalin, T. Williams

Imperial College, London, U.K.
G. Auzinger, R. Bainbridge, J. Borg, S. Breeze, O. Buchmuller, A. Bundock, S. Casasso, M. Citron, D. Colling, L. Corpe, P. Dauncey, G. Davies, A. De Wit, M. Della Negra, R. Di Maria, A. Elwood, Y. Haddad, G. Hall, G. Iles, T. James, R. Lane, C. Laner, L. Lyons,

A.-M. Magnan, S. Malik, L. Mastrolorenzo, T. Matsushita, J. Nash, A. Nikitenko[7], V. Palladino, M. Pesaresi, D.M. Raymond, A. Richards, A. Rose, E. Scott, C. Seez, A. Shtipliyski, S. Summers, A. Tapper, K. Uchida, M. Vazquez Acosta[64], T. Virdee[16], N. Wardle, D. Winterbottom, J. Wright, S.C. Zenz

Brunel University, Uxbridge, U.K.

J.E. Cole, P.R. Hobson, A. Khan, P. Kyberd, I.D. Reid, L. Teodorescu, M. Turner, S. Zahid

Baylor University, Waco, U.S.A.

A. Borzou, K. Call, J. Dittmann, K. Hatakeyama, H. Liu, N. Pastika, C. Smith

Catholic University of America, Washington DC, U.S.A.

R. Bartek, A. Dominguez

The University of Alabama, Tuscaloosa, U.S.A.

A. Buccilli, S.I. Cooper, C. Henderson, P. Rumerio, C. West

Boston University, Boston, U.S.A.

D. Arcaro, A. Avetisyan, T. Bose, D. Gastler, D. Rankin, C. Richardson, J. Rohlf, L. Sulak, D. Zou

Brown University, Providence, U.S.A.

G. Benelli, D. Cutts, A. Garabedian, M. Hadley, J. Hakala, U. Heintz, J.M. Hogan, K.H.M. Kwok, E. Laird, G. Landsberg, J. Lee, Z. Mao, M. Narain, J. Pazzini, S. Piperov, S. Sagir, R. Syarif, D. Yu

University of California, Davis, Davis, U.S.A.

R. Band, C. Brainerd, R. Breedon, D. Burns, M. Calderon De La Barca Sanchez, M. Chertok, J. Conway, R. Conway, P.T. Cox, R. Erbacher, C. Flores, G. Funk, W. Ko, R. Lander, C. Mclean, M. Mulhearn, D. Pellett, J. Pilot, S. Shalhout, M. Shi, J. Smith, D. Stolp, K. Tos, M. Tripathi, Z. Wang

University of California, Los Angeles, U.S.A.

M. Bachtis, C. Bravo, R. Cousins, A. Dasgupta, A. Florent, J. Hauser, M. Ignatenko, N. Mccoll, S. Regnard, D. Saltzberg, C. Schnaible, V. Valuev

University of California, Riverside, Riverside, U.S.A.

E. Bouvier, K. Burt, R. Clare, J. Ellison, J.W. Gary, S.M.A. Ghiasi Shirazi, G. Hanson, J. Heilman, G. Karapostoli, E. Kennedy, F. Lacroix, O.R. Long, M. Olmedo Negrete, M.I. Paneva, W. Si, L. Wang, H. Wei, S. Wimpenny, B. R. Yates

University of California, San Diego, La Jolla, U.S.A.

J.G. Branson, S. Cittolin, M. Derdzinski, R. Gerosa, D. Gilbert, B. Hashemi, A. Holzner, D. Klein, G. Kole, V. Krutelyov, J. Letts, I. Macneill, M. Masciovecchio, D. Olivito, S. Padhi, M. Pieri, M. Sani, V. Sharma, S. Simon, M. Tadel, A. Vartak, S. Wasserbaech[65], J. Wood, F. Würthwein, A. Yagil, G. Zevi Della Porta

University of California, Santa Barbara - Department of Physics, Santa Barbara, U.S.A.

N. Amin, R. Bhandari, J. Bradmiller-Feld, C. Campagnari, A. Dishaw, V. Dutta, M. Franco Sevilla, F. Golf, L. Gouskos, R. Heller, J. Incandela, A. Ovcharova, H. Qu, J. Richman, D. Stuart, I. Suarez, J. Yoo

California Institute of Technology, Pasadena, U.S.A.

D. Anderson, A. Bornheim, J.M. Lawhorn, H.B. Newman, T. Nguyen, C. Pena, M. Spiropulu, J.R. Vlimant, S. Xie, Z. Zhang, R.Y. Zhu

Carnegie Mellon University, Pittsburgh, U.S.A.

M.B. Andrews, T. Ferguson, T. Mudholkar, M. Paulini, J. Russ, M. Sun, H. Vogel, I. Vorobiev, M. Weinberg

University of Colorado Boulder, Boulder, U.S.A.

J.P. Cumalat, W.T. Ford, F. Jensen, A. Johnson, M. Krohn, S. Leontsinis, T. Mulholland, K. Stenson, S.R. Wagner

Cornell University, Ithaca, U.S.A.

J. Alexander, J. Chaves, J. Chu, S. Dittmer, K. Mcdermott, N. Mirman, J.R. Patterson, D. Quach, A. Rinkevicius, A. Ryd, L. Skinnari, L. Soffi, S.M. Tan, Z. Tao, J. Thom, J. Tucker, P. Wittich, M. Zientek

Fermi National Accelerator Laboratory, Batavia, U.S.A.

S. Abdullin, M. Albrow, M. Alyari, G. Apollinari, A. Apresyan, A. Apyan, S. Banerjee, L.A.T. Bauerdick, A. Beretvas, J. Berryhill, P.C. Bhat, G. Bolla[†], K. Burkett, J.N. Butler, A. Canepa, G.B. Cerati, H.W.K. Cheung, F. Chlebana, M. Cremonesi, J. Duarte, V.D. Elvira, J. Freeman, Z. Gecse, E. Gottschalk, L. Gray, D. Green, S. Grünendahl, O. Gutsche, R.M. Harris, S. Hasegawa, J. Hirschauer, Z. Hu, B. Jayatilaka, S. Jindariani, M. Johnson, U. Joshi, B. Klima, B. Kreis, S. Lammel, D. Lincoln, R. Lipton, M. Liu, T. Liu, R. Lopes De Sá, J. Lykken, K. Maeshima, N. Magini, J.M. Marraffino, D. Mason, P. McBride, P. Merkel, S. Mrenna, S. Nahn, V. O'Dell, K. Pedro, O. Prokofyev, G. Rakness, L. Ristori, B. Schneider, E. Sexton-Kennedy, A. Soha, W.J. Spalding, L. Spiegel, S. Stoynev, J. Strait, N. Strobbe, L. Taylor, S. Tkaczyk, N.V. Tran, L. Uplegger, E.W. Vaandering, C. Vernieri, M. Verzocchi, R. Vidal, M. Wang, H.A. Weber, A. Whitbeck

University of Florida, Gainesville, U.S.A.

D. Acosta, P. Avery, P. Bortignon, D. Bourilkov, A. Brinkerhoff, A. Carnes, M. Carver, D. Curry, R.D. Field, I.K. Furic, S.V. Gleyzer, B.M. Joshi, J. Konigsberg, A. Korytov, K. Kotov, P. Ma, K. Matchev, H. Mei, G. Mitselmakher, D. Rank, K. Shi, D. Sperka, N. Terentyev, L. Thomas, J. Wang, S. Wang, J. Yelton

Florida International University, Miami, U.S.A.

Y.R. Joshi, S. Linn, P. Markowitz, J.L. Rodriguez

Florida State University, Tallahassee, U.S.A.

A. Ackert, T. Adams, A. Askew, S. Hagopian, V. Hagopian, K.F. Johnson, T. Kolberg, G. Martinez, T. Perry, H. Prosper, A. Saha, A. Santra, V. Sharma, R. Yohay

JHEP03(2018)160

Florida Institute of Technology, Melbourne, U.S.A.
M.M. Baarmand, V. Bhopatkar, S. Colafranceschi, M. Hohlmann, D. Noonan, T. Roy, F. Yumiceva

University of Illinois at Chicago (UIC), Chicago, U.S.A.
M.R. Adams, L. Apanasevich, D. Berry, R.R. Betts, R. Cavanaugh, X. Chen, O. Evdokimov, C.E. Gerber, D.A. Hangal, D.J. Hofman, K. Jung, J. Kamin, I.D. Sandoval Gonzalez, M.B. Tonjes, H. Trauger, N. Varelas, H. Wang, Z. Wu, J. Zhang

The University of Iowa, Iowa City, U.S.A.
B. Bilki[66], W. Clarida, K. Dilsiz[67], S. Durgut, R.P. Gandrajula, M. Haytmyradov, V. Khristenko, J.-P. Merlo, H. Mermerkaya[68], A. Mestvirishvili, A. Moeller, J. Nachtman, H. Ogul[69], Y. Onel, F. Ozok[70], A. Penzo, C. Snyder, E. Tiras, J. Wetzel, K. Yi

Johns Hopkins University, Baltimore, U.S.A.
B. Blumenfeld, A. Cocoros, N. Eminizer, D. Fehling, L. Feng, A.V. Gritsan, P. Maksimovic, J. Roskes, U. Sarica, M. Swartz, M. Xiao, C. You

The University of Kansas, Lawrence, U.S.A.
A. Al-bataineh, P. Baringer, A. Bean, S. Boren, J. Bowen, J. Castle, S. Khalil, A. Kropivnitskaya, D. Majumder, W. Mcbrayer, M. Murray, C. Royon, S. Sanders, E. Schmitz, J.D. Tapia Takaki, Q. Wang

Kansas State University, Manhattan, U.S.A.
A. Ivanov, K. Kaadze, Y. Maravin, A. Mohammadi, L.K. Saini, N. Skhirtladze, S. Toda

Lawrence Livermore National Laboratory, Livermore, U.S.A.
F. Rebassoo, D. Wright

University of Maryland, College Park, U.S.A.
C. Anelli, A. Baden, O. Baron, A. Belloni, S.C. Eno, Y. Feng, C. Ferraioli, N.J. Hadley, S. Jabeen, G.Y. Jeng, R.G. Kellogg, J. Kunkle, A.C. Mignerey, F. Ricci-Tam, Y.H. Shin, A. Skuja, S.C. Tonwar

Massachusetts Institute of Technology, Cambridge, U.S.A.
D. Abercrombie, B. Allen, V. Azzolini, R. Barbieri, A. Baty, R. Bi, S. Brandt, W. Busza, I.A. Cali, M. D'Alfonso, Z. Demiragli, G. Gomez Ceballos, M. Goncharov, D. Hsu, M. Hu, Y. Iiyama, G.M. Innocenti, M. Klute, D. Kovalskyi, Y.S. Lai, Y.-J. Lee, A. Levin, P.D. Luckey, B. Maier, A.C. Marini, C. Mcginn, C. Mironov, S. Narayanan, X. Niu, C. Paus, C. Roland, G. Roland, J. Salfeld-Nebgen, G.S.F. Stephans, K. Tatar, D. Velicanu, J. Wang, T.W. Wang, B. Wyslouch

University of Minnesota, Minneapolis, U.S.A.
A.C. Benvenuti, R.M. Chatterjee, A. Evans, P. Hansen, J. Hiltbrand, S. Kalafut, Y. Kubota, Z. Lesko, J. Mans, S. Nourbakhsh, N. Ruckstuhl, R. Rusack, J. Turkewitz, M.A. Wadud

University of Mississippi, Oxford, U.S.A.
J.G. Acosta, S. Oliveros

JHEP03(2018)160

University of Nebraska-Lincoln, Lincoln, U.S.A.

E. Avdeeva, K. Bloom, D.R. Claes, C. Fangmeier, R. Gonzalez Suarez, R. Kamalieddin, I. Kravchenko, J. Monroy, J.E. Siado, G.R. Snow, B. Stieger

State University of New York at Buffalo, Buffalo, U.S.A.

J. Dolen, A. Godshalk, C. Harrington, I. Iashvili, D. Nguyen, A. Parker, S. Rappoccio, B. Roozbahani

Northeastern University, Boston, U.S.A.

G. Alverson, E. Barberis, A. Hortiangtham, A. Massironi, D.M. Morse, T. Orimoto, R. Teixeira De Lima, D. Trocino, D. Wood

Northwestern University, Evanston, U.S.A.

S. Bhattacharya, O. Charaf, K.A. Hahn, N. Mucia, N. Odell, M.H. Schmitt, K. Sung, M. Trovato, M. Velasco

University of Notre Dame, Notre Dame, U.S.A.

N. Dev, M. Hildreth, K. Hurtado Anampa, C. Jessop, D.J. Karmgard, N. Kellams, K. Lannon, W. Li, N. Loukas, N. Marinelli, F. Meng, C. Mueller, Y. Musienko[37], M. Planer, A. Reinsvold, R. Ruchti, P. Siddireddy, G. Smith, S. Taroni, M. Wayne, A. Wightman, M. Wolf, A. Woodard

The Ohio State University, Columbus, U.S.A.

J. Alimena, L. Antonelli, B. Bylsma, L.S. Durkin, S. Flowers, B. Francis, A. Hart, C. Hill, W. Ji, B. Liu, W. Luo, B.L. Winer, H.W. Wulsin

Princeton University, Princeton, U.S.A.

S. Cooperstein, O. Driga, P. Elmer, J. Hardenbrook, P. Hebda, S. Higginbotham, A. Kalogeropoulos, D. Lange, J. Luo, D. Marlow, K. Mei, I. Ojalvo, J. Olsen, C. Palmer, P. Piroué, D. Stickland, C. Tully

University of Puerto Rico, Mayaguez, U.S.A.

S. Malik, S. Norberg

Purdue University, West Lafayette, U.S.A.

A. Barker, V.E. Barnes, S. Das, S. Folgueras, L. Gutay, M.K. Jha, M. Jones, A.W. Jung, A. Khatiwada, D.H. Miller, N. Neumeister, C.C. Peng, H. Qiu, J.F. Schulte, J. Sun, F. Wang, W. Xie

Purdue University Northwest, Hammond, U.S.A.

T. Cheng, N. Parashar, J. Stupak

Rice University, Houston, U.S.A.

A. Adair, Z. Chen, K.M. Ecklund, S. Freed, F.J.M. Geurts, M. Guilbaud, M. Kilpatrick, W. Li, B. Michlin, M. Northup, B.P. Padley, J. Roberts, J. Rorie, W. Shi, Z. Tu, J. Zabel, A. Zhang

JHEP03(2018)160

University of Rochester, Rochester, U.S.A.
A. Bodek, P. de Barbaro, R. Demina, Y.t. Duh, T. Ferbel, M. Galanti, A. Garcia-Bellido, J. Han, O. Hindrichs, A. Khukhunaishvili, K.H. Lo, P. Tan, M. Verzetti

The Rockefeller University, New York, U.S.A.
R. Ciesielski, K. Goulianos, C. Mesropian

Rutgers, The State University of New Jersey, Piscataway, U.S.A.
A. Agapitos, J.P. Chou, Y. Gershtein, T.A. Gómez Espinosa, E. Halkiadakis, M. Heindl, E. Hughes, S. Kaplan, R. Kunnawalkam Elayavalli, S. Kyriacou, A. Lath, R. Montalvo, K. Nash, M. Osherson, H. Saka, S. Salur, S. Schnetzer, D. Sheffield, S. Somalwar, R. Stone, S. Thomas, P. Thomassen, M. Walker

University of Tennessee, Knoxville, U.S.A.
A.G. Delannoy, M. Foerster, J. Heideman, G. Riley, K. Rose, S. Spanier, K. Thapa

Texas A&M University, College Station, U.S.A.
O. Bouhali[71], A. Castaneda Hernandez[71], A. Celik, M. Dalchenko, M. De Mattia, A. Delgado, S. Dildick, R. Eusebi, J. Gilmore, T. Huang, T. Kamon[72], R. Mueller, Y. Pakhotin, R. Patel, A. Perloff, L. Perniè, D. Rathjens, A. Safonov, A. Tatarinov, K.A. Ulmer

Texas Tech University, Lubbock, U.S.A.
N. Akchurin, J. Damgov, F. De Guio, P.R. Dudero, J. Faulkner, E. Gurpinar, S. Kunori, K. Lamichhane, S.W. Lee, T. Libeiro, T. Mengke, S. Muthumuni, T. Peltola, S. Undleeb, I. Volobouev, Z. Wang

Vanderbilt University, Nashville, U.S.A.
S. Greene, A. Gurrola, R. Janjam, W. Johns, C. Maguire, A. Melo, H. Ni, K. Padeken, P. Sheldon, S. Tuo, J. Velkovska, Q. Xu

University of Virginia, Charlottesville, U.S.A.
M.W. Arenton, P. Barria, B. Cox, R. Hirosky, M. Joyce, A. Ledovskoy, H. Li, C. Neu, T. Sinthuprasith, Y. Wang, E. Wolfe, F. Xia

Wayne State University, Detroit, U.S.A.
R. Harr, P.E. Karchin, N. Poudyal, J. Sturdy, P. Thapa, S. Zaleski

University of Wisconsin - Madison, Madison, WI, U.S.A.
M. Brodski, J. Buchanan, C. Caillol, S. Dasu, L. Dodd, S. Duric, B. Gomber, M. Grothe, M. Herndon, A. Hervé, U. Hussain, P. Klabbers, A. Lanaro, A. Levine, K. Long, R. Loveless, T. Ruggles, A. Savin, N. Smith, W.H. Smith, D. Taylor, N. Woods

†: Deceased
1: Also at Vienna University of Technology, Vienna, Austria
2: Also at State Key Laboratory of Nuclear Physics and Technology, Peking University, Beijing, China
3: Also at IRFU, CEA, Université Paris-Saclay, Gif-sur-Yvette, France
4: Also at Universidade Estadual de Campinas, Campinas, Brazil

5: Also at Universidade Federal de Pelotas, Pelotas, Brazil
6: Also at Université Libre de Bruxelles, Bruxelles, Belgium
7: Also at Institute for Theoretical and Experimental Physics, Moscow, Russia
8: Also at Joint Institute for Nuclear Research, Dubna, Russia
9: Also at Helwan University, Cairo, Egypt
10: Now at Zewail City of Science and Technology, Zewail, Egypt
11: Now at Fayoum University, El-Fayoum, Egypt
12: Also at British University in Egypt, Cairo, Egypt
13: Now at Ain Shams University, Cairo, Egypt
14: Also at Université de Haute Alsace, Mulhouse, France
15: Also at Skobeltsyn Institute of Nuclear Physics, Lomonosov Moscow State University, Moscow, Russia
16: Also at CERN, European Organization for Nuclear Research, Geneva, Switzerland
17: Also at RWTH Aachen University, III. Physikalisches Institut A, Aachen, Germany
18: Also at University of Hamburg, Hamburg, Germany
19: Also at Brandenburg University of Technology, Cottbus, Germany
20: Also at MTA-ELTE Lendület CMS Particle and Nuclear Physics Group, Eötvös Loránd University, Budapest, Hungary
21: Also at Institute of Nuclear Research ATOMKI, Debrecen, Hungary
22: Also at Institute of Physics, University of Debrecen, Debrecen, Hungary
23: Also at Indian Institute of Technology Bhubaneswar, Bhubaneswar, India
24: Also at Institute of Physics, Bhubaneswar, India
25: Also at University of Visva-Bharati, Santiniketan, India
26: Also at University of Ruhuna, Matara, Sri Lanka
27: Also at Isfahan University of Technology, Isfahan, Iran
28: Also at Yazd University, Yazd, Iran
29: Also at Plasma Physics Research Center, Science and Research Branch, Islamic Azad University, Tehran, Iran
30: Also at Università degli Studi di Siena, Siena, Italy
31: Also at INFN Sezione di Milano-Bicocca; Università di Milano-Bicocca, Milano, Italy
32: Also at Purdue University, West Lafayette, U.S.A.
33: Also at International Islamic University of Malaysia, Kuala Lumpur, Malaysia
34: Also at Malaysian Nuclear Agency, MOSTI, Kajang, Malaysia
35: Also at Consejo Nacional de Ciencia y Tecnología, Mexico city, Mexico
36: Also at Warsaw University of Technology, Institute of Electronic Systems, Warsaw, Poland
37: Also at Institute for Nuclear Research, Moscow, Russia
38: Now at National Research Nuclear University 'Moscow Engineering Physics Institute' (MEPhI), Moscow, Russia
39: Also at St. Petersburg State Polytechnical University, St. Petersburg, Russia
40: Also at University of Florida, Gainesville, U.S.A.
41: Also at P.N. Lebedev Physical Institute, Moscow, Russia
42: Also at California Institute of Technology, Pasadena, U.S.A.
43: Also at Budker Institute of Nuclear Physics, Novosibirsk, Russia
44: Also at Faculty of Physics, University of Belgrade, Belgrade, Serbia
45: Also at University of Belgrade, Faculty of Physics and Vinca Institute of Nuclear Sciences, Belgrade, Serbia
46: Also at Scuola Normale e Sezione dell'INFN, Pisa, Italy
47: Also at National and Kapodistrian University of Athens, Athens, Greece

JHEP03(2018)160

48: Also at Riga Technical University, Riga, Latvia
49: Also at Universität Zürich, Zurich, Switzerland
50: Also at Stefan Meyer Institute for Subatomic Physics (SMI), Vienna, Austria
51: Also at Gaziosmanpasa University, Tokat, Turkey
52: Also at Istanbul Aydin University, Istanbul, Turkey
53: Also at Mersin University, Mersin, Turkey
54: Also at Cag University, Mersin, Turkey
55: Also at Piri Reis University, Istanbul, Turkey
56: Also at Adiyaman University, Adiyaman, Turkey
57: Also at Izmir Institute of Technology, Izmir, Turkey
58: Also at Necmettin Erbakan University, Konya, Turkey
59: Also at Marmara University, Istanbul, Turkey
60: Also at Kafkas University, Kars, Turkey
61: Also at Istanbul Bilgi University, Istanbul, Turkey
62: Also at Rutherford Appleton Laboratory, Didcot, U.K.
63: Also at School of Physics and Astronomy, University of Southampton, Southampton, U.K.
64: Also at Instituto de Astrofísica de Canarias, La Laguna, Spain
65: Also at Utah Valley University, Orem, U.S.A.
66: Also at Beykent University, Istanbul, Turkey
67: Also at Bingol University, Bingol, Turkey
68: Also at Erzincan University, Erzincan, Turkey
69: Also at Sinop University, Sinop, Turkey
70: Also at Mimar Sinan University, Istanbul, Istanbul, Turkey
71: Also at Texas A&M University at Qatar, Doha, Qatar
72: Also at Kyungpook National University, Daegu, Koreae

JHEP03(2018)160